Transportation Research Interdisciplinary Perspectives 39 (2026) 102136

Contents lists available at ScienceDirect

Transportation Research Interdisciplinary Perspectives

journal homepage: www.elsevier.com/locate/trip

Predicting vessel arrival time in inland waterways: Integrating ETA, AIS, and traffic flow data

Peter Wenzel [a,1], Zhong Chu [b,c,*,2,3], Frederik Schulte [b,4]

[a] Institute of Information Systems, University of Hamburg, Hamburg, Germany
[b] Department of Maritime and Transport Technology, Delft University of Technology, Delft, Netherlands
[c] Department of Logistics and Maritime Studies, The Hong Kong Polytechnic University, Hong Kong, China

ARTICLE INFO

Keywords:
Inland waterway transportation
Vessel arrival time prediction
Vessel traffic flow
Port operation

ABSTRACT

The prediction of vessel arrival time (VAT) is crucial for port operations, which depend on vessel-reported estimated arrival time (ETA) for scheduling. However, discrepancies between ETA and actual arrival time often undermine planning reliability, causing inefficiencies and economic losses. Unlike ocean shipping, inland waterway transportation (IWT) faces distinct challenges such as fixed routes and dense vessel traffic. Existing VAT studies mainly focus on maritime transport and typically use single data sources (e.g., AIS or port call data), overlooking key IWT characteristics like structured routes and high traffic intensity. To address this gap, we propose a novel framework that integrates multiple data sources, including port call records, AIS trajectories, vessel features for VAT prediction. A tailored feature engineering pipeline reconstructs vessel routes and estimates sailing distances and traffic flow. Using the Port of Rotterdam as a case study, advanced ensemble tree-based models are applied. Experimental results show a 79.55% reduction in mean absolute error (from 17.06 to 3.49 h) relative to vessel-reported ETAs. Feature importance analysis identifies voyage distance, reported ETA, and waterway traffic flow as key factors. This study demonstrates that data-driven VAT prediction can support proactive berth scheduling, traffic-aware coordination, and just-in-time vessel arrivals, thereby improving operational efficiency, reducing emissions in IWT, and supporting sustainable port management.

1. Introduction

Global shipping is facing growing pressure to decarbonize, making operational efficiency an important and practical means of reducing fuel consumption and associated emissions (Saafi et al., 2025). In this context, efficient maritime logistics relies on close coordination between vessel and port operations, and accurate estimation of vessel arrival time (ETA) is therefore crucial for voyage planning, berth scheduling, and cargo handling (Halpe et al., 2025; Ta et al., 2025). As the basis for all subsequent port-related decisions, inaccuracies in ETA predictions can propagate throughout the logistics chain, disrupting berth allocation, yard operations, and hinterland transportation (Nosar, 2025). Such deviations often lead to resource underutilization, prolonged turnaround times, and increased costs, including demurrage and detention charges. Unlike urban traffic forecasting, vessel arrival time (VAT) prediction spans longer temporal horizons and is subject to greater uncertainty due to changing weather conditions, dynamic navigational decisions en route, and fluctuating port congestion. These complexities underscore the need for more robust and adaptive predictive models capable of capturing delay-inducing factors and supporting reliable port scheduling.

Numerous studies have explored artificial intelligence (AI)-based approaches for VAT prediction under uncertainty, mainly focusing on ocean-going vessels (Jiang et al., 2025; Perra and Boile, 2026). These approaches typically rely on either static port call records (e.g., ETA and actual time of arrival (ATA)) or dynamic automatic identification system (AIS) data that continuously track vessel position, speed, and heading. While port call data provide operational timestamps, AIS data enable real-time navigation monitoring. However, most existing studies adopt a single data source and often neglect contextual variables such as vessel specifications, meteorological conditions, and port traffic levels. This limited data integration constrains the models'

* Corresponding author at: Department of Maritime and Transport Technology, Delft University of Technology, Delft, Netherlands.
E-mail addresses: P.A.Wenzel@rsm.nl (P. Wenzel), zhongchu@polyu.edu.hk (Z. Chu), F.Schulte@tudelft.nl (F. Schulte).

[1] Research Staff.
[2] Co-first author.
[3] Research Fellow.
[4] Associated Professor.

https://doi.org/10.1016/j.trip.2026.102136
Received 27 November 2025; Received in revised form 25 June 2026; Accepted 4 July 2026
Available online 13 July 2026

capacity to reflect the full complexity of maritime navigation. As highlighted in recent literature (Li et al., 2023a; Jiang et al., 2025; Chu et al., 2026), one major shortcoming is the insufficient incorporation of heterogeneous data sources beyond AIS, which hinders both the predictive accuracy and robustness of current approaches. Moreover, VAT prediction in inland waterway transportation (IWT) has received comparatively little attention. Existing methods often directly transplant techniques developed for ocean-going contexts, overlooking the distinct operational characteristics and automation requirements of inland navigation. Compared with ocean shipping, where vessels generally travel along relatively open routes with greater navigational flexibility and where arrival prediction is often dominated by large-scale voyage planning, weather conditions, and destination port congestion, inland waterway shipping operates in a far more constrained and infrastructure-dependent environment. Vessel movements in IWT are tightly constrained by narrow channels, fixed sailing lanes, lock systems, bridge crossings, and dense reporting points, while also being exposed to frequent traffic interactions and localized operational disturbances. Unlike open-sea navigation, inland vessel traffic often exhibits pronounced microscopic interaction patterns, such as vessel-following behavior and non-free-flow conditions. Recent studies based on vessel-following experiments in inland restricted waterways have shown that inland vessels may form following queues and that their motion can be described by adapted car-following or vessel-following models (Yang et al., 2023; Jin et al., 2023). In addition, multi-source observations of inland restricted waterways reveal systematic relationships among vessel speed, spacing, density, and flow rate, indicating that inland traffic states are strongly affected by local channel conditions and surrounding traffic environments (W. Yang et al., 2025). These findings suggest that VAT prediction in IWT should account not only for vessel-specific sailing progress but also for short-term traffic interactions and local operational contexts. As a result, inland navigation requires more fine-grained, short-term, and context-aware prediction to support automated or data-driven decision-making. Even small deviations in arrival time may quickly propagate into lock delays, berth conflicts, and downstream scheduling disruptions. This requirement is further amplified by the fact that inland ports are typically smaller and more numerous, with shorter inter-port distances and higher berth turnover rates, making accurate and dedicated VAT prediction particularly important. At the same time, the constrained topology of inland waterways and the availability of frequent reporting points make it feasible to estimate remaining sailing distances with relatively high precision and to monitor local traffic conditions in near real time. These characteristics highlight both the urgency and the feasibility of developing dedicated VAT prediction models for inland waterway systems, rather than simply adapting methods originally designed for open-sea transport.

To address the identified research gaps, this study proposes a novel machine learning-based framework to predict VAT in IWT, with a case study focused on the port of Rotterdam. The proposed approach integrates heterogeneous data sources, including vessel-reported ETA, meteorological conditions (e.g., temperature, wind speed and direction, and water levels), vessel specifications (e.g., length and width), and AIS data. In this study, the prediction framework is developed under several practical assumptions to reflect the operational characteristics of inland waterway transportation. First, vessels are assumed to travel along the fixed and navigable topology of the inland waterway network, such that their feasible movement paths can be reasonably approximated based on historical AIS trajectories and waterway connectivity. Second, although vessel operations in practice may still be influenced by dispatching decisions and human intervention, the framework mainly focuses on routine operational conditions and does not explicitly model irregular extreme interventions or highly exceptional disruptions. Third, the proposed framework assumes that the main factors affecting VAT can be captured through observable vessel, environmental, and traffic-related variables.

To accurately capture the spatial dynamics of inland navigation, the proposed framework innovatively applies the A* search algorithm to estimate the remaining sailing distance based on the fixed topology of the waterway network. It also integrates real-time traffic flow information to account for dynamic congestion and operational delays, thereby enabling a more context-aware and accurate VAT prediction.

The proposed approach leverages advanced tree-based machine learning models, including eXtreme Gradient Boosting (XGBoost) and Light Gradient Boosting Machine (LightGBM), for VAT prediction. When evaluated using a chronologically ordered data split, the model achieves a substantial reduction in the prediction error, lowering the mean absolute error (MAE) by 79.55% (from 17.06 to 3.49 h) and the root mean square error (RMSE) by 63.22% (from 29.99 to 11.03 h), compared to the vessel-reported ETAs. These results demonstrate the effectiveness of the model in capturing complex vessel arrival patterns in inland waterways. In summary, this paper makes four specific contributions:

1. It introduces a practical VAT prediction framework for inland waterway vessels, shifting the focus beyond traditional ocean-going applications.
2. It suggests an A* algorithm for precisely segmenting the navigation route, enhancing the accuracy of the remaining vessel travel distance calculations and evaluating the maritime traffic flow;
3. It integrates several novel features for VAT prediction, including ETA and AIS records, vessel remaining voyage distance, maritime traffic flow, environmental conditions, and vessel physical dimensions;
4. It evaluates multiple prediction models on real-world vessel arrival data and derives new insights from feature correlation and importance analysis based on VAT prediction models;

Fig. 1 illustrates the flowchart of our proposed method for estimating VAT within IWT. In the initial stage, raw AIS data and supplementary datasets are systematically processed to generate a structured set of features. This involves a series of procedures, including AIS data cleaning, vessel trajectory reconstruction, punctuality evaluation, inland waterway segmentation, traffic flow estimation, and feature extension. The second stage focuses on VAT prediction, where both state-of-the-art tree-based models and neural networks are employed. In the final stage, we conduct a comprehensive prediction result analysis, including a quantitative assessment of predicted VAT and a feature importance evaluation using SHapley Additive exPlanations (SHAP) values. The performance of different models is compared using metrics such as RMSE, MAE, median absolute deviation (MAD), and R-squared (R^2), providing insights for further discussion and model interpretation. In addition to improving predictive accuracy, this study also aims to bridge the gap between data-driven modeling and practical decision-making by deriving managerial and policy implications that support more efficient, coordinated, and sustainable inland waterway operations.

The remainder of this paper is organized as follows. Section 2 reviews the existing literature on VAT prediction and highlights the current research gaps. Section 3 describes the data processing pipeline for vessel arrival data, the integration of heterogeneous data sources, and the analysis of the punctuality of vessel arrival records. In Section 4, the predictive models are introduced and applied to VAT forecasting, followed by an analysis of the relative importance of features influencing VAT predictions, along with a discussion of the insights and practical implications of the results. Finally, Section 6 concludes the study and outlines the directions for future research.

2. Literature review

Accurate prediction of Vessel Arrival Time (VAT) is essential for enhancing the efficiency of maritime logistics and port operations,

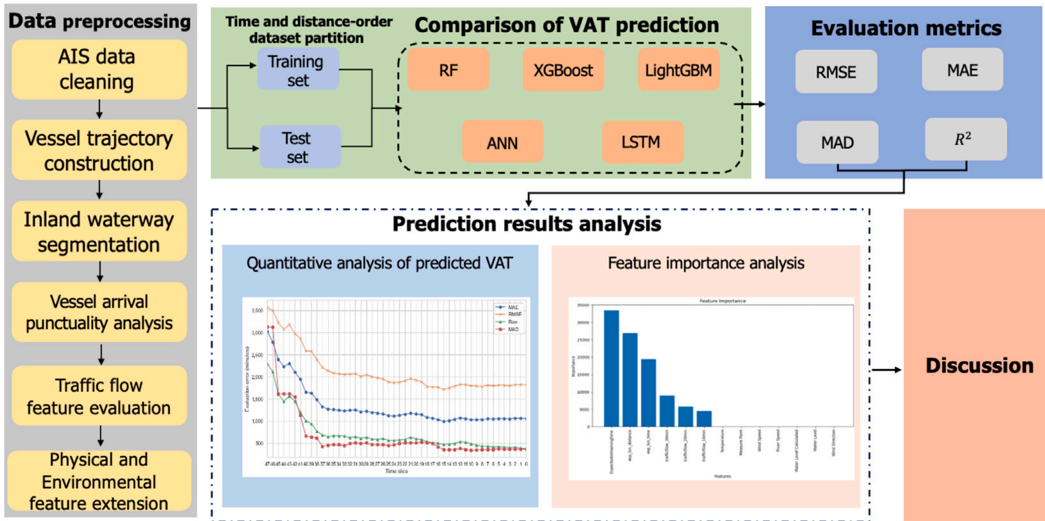

Fig. 1. Flowchart of the evaluation and prediction process.

particularly in the face of growing global trade volumes and increasing port congestion (Filom et al., 2022). To mitigate the uncertainty associated with vessel arrivals, a substantial body of research has been devoted to developing predictive models that support data-driven operational decisions. Existing studies on VAT prediction can be broadly classified into two main approaches: feature engineering-based methods and trajectory-based methods (Jiang et al., 2025; Chu et al., 2025). The first approach is trajectory-based, which involves predicting the vessel's future path to its destination and then estimating the remaining travel time accordingly. This method explicitly captures the spatiotemporal dynamics of vessel movements but typically relies on dense and continuous AIS sequences for accurate path reconstruction. The second approach is feature engineering-based, which directly forecasts VAT from structured input features after data preprocessing. Each instance is mapped to a predicted VAT, making this approach particularly suitable for large-scale regression tasks.

2.1. Using vessel trajectory for VAT prediction

Predicting VAT through vessel trajectory involves a two-stage process: reconstructing the vessel's expected path and subsequently estimating the arrival time based on this trajectory. In this approach, raw AIS data are first preprocessed to reconstruct historical or real-time vessel trajectories, capturing spatial and temporal movement patterns. For each individual voyage, the model then estimates VAT by leveraging trajectory-specific information, such as current position, speed, and navigational route (Jiang et al., 2025; Lei et al., 2024).

In early studies, Kim et al. (2017) employ statistical analysis to predict vessel trajectories by modeling average speeds with a Gaussian distribution, resulting in a significant improvement in the accuracy of VAT calculations. Similarly, Last et al. (2019) preprocess historical AIS data, construct a dynamic network of vessel movements, and apply traditional machine learning models, such as decision trees, to forecast future trajectories and VAT. They also develop an interactive visualization tool that enables real-time analysis of vessel movement predictions, offering valuable support for maritime logistics and port operations. In 2021, Ogura et al. (2021) integrate AIS data with future weather forecasts into a Bayesian reasoning framework to estimate vessel trajectories and sailing speeds. This method enhances the accuracy of VAT prediction by dynamically accounting for environmental conditions.

Furthermore, Park et al. (2021) employ reinforcement learning to reconstruct vessel trajectories and apply Bayesian sampling to estimate vessel speeds and ETA, providing a robust approach for accurate VAT prediction. Xu et al. (2022) perform statistical analysis to cluster vessel trajectories based on similarities in movement characteristics and apply a regression model to estimate VAT within each cluster. The model demonstrates superior performance when evaluated using AIS data from the Port of Rotterdam. In 2023, the field advances significantly with the work of Kim et al. (2023)., who propose a big data approach by restructuring large-scale international vessel trajectory sequences into a nested format. They develop a neural network model specifically designed for long-term destination prediction, enabling forecast horizons of several days (Kim et al., 2023).

Li et al. (2023b) conduct a comprehensive review of recent ship trajectory prediction algorithms, systematically evaluating deep learning models in terms of predictive accuracy, computational efficiency, and applicability to IWT scenarios. Their study highlights two key research gaps: the limited adoption of multimodel methodologies and the insufficient exploration of multisource data fusion. Emmens et al. (2021) examine the advantages and limitations of utilizing AIS data in the context of inland waterway transport. By analyzing AIS records from the Amsterdam region and conducting interviews with industry stakeholders, they identify missing and erroneous data as the primary challenges limiting the effective application of AIS in inland navigation. Li et al. (2023a) provide a comprehensive exploration of vessel trajectory prediction across both inland and ocean-going contexts, with particular emphasis on short-term vessel trajectories forecasting. Their review underscores the pivotal role of AIS data in enhancing predictive accuracy. By systematically analyzing existing literature, the authors trace the evolution of predictive methodologies from traditional data mining techniques to advanced machine learning approaches (Li et al., 2023a).

Despite notable progress in VAT prediction using vessel trajectory modeling, several limitations remain. Most existing models require a fixed number of AIS data points as input, leading researchers to interpolate and standardize trajectory lengths during preprocessing (Qiang et al., 2023; Li et al., 2023a). However, in real-world port operations, AIS data obtained by port authorities often vary significantly in trajectory length, which increases data processing complexity and hinders practical implementation. Moreover, trajectory-based VAT prediction methods are typically confined to short-range forecasting, spanning only a few kilometers, which offers limited operational value. For port authorities, the primary interest lies in long-range VAT prediction, enabling proactive berth scheduling and traffic management.

2.2. Data engineering for VAT prediction

VAT prediction based on data engineering directly estimates VAT by extracting and preprocessing relevant features from raw AIS and related datasets. Each entry in the structured dataset has a corresponding predicted VAT value. Unlike trajectory-based methods, which require path reconstruction and primarily focus on short-distance predictions, data engineering models frame VAT estimation is more suitable for long-distance and long-horizon forecasting (Jiang et al., 2025). Building on data mining, Kim et al. develop a model that integrates AIS data processing with a classification and regression tree (CART) algorithm, embedded within a case-based reasoning framework, to identify potential delays in vessel arrival. The approach leverages both real-time tracking and historical AIS data to improve predictive accuracy (Kim et al., 2017).

In 2020, the field advanced with the work of Wu et al. (2020), who propose a novel approach for estimating vessel arrival and departure times in narrow waterways, as well as calculating travel durations between docks and predefined reference points. Štepec et al. (2020) present an innovative approach that leverages multiple years of historical AIS data to predict vessel turnaround times at the Port of Bordeaux, demonstrating the potential of machine learning for enhancing port efficiency. Furthermore, Viellechner and Spinler (2020) conduct a comprehensive study on vessel delay prediction by evaluating multiple machine learning algorithms, utilizing a high-dimensional feature set extracted from AIS data. In 2021, Noman et al. (2021) conduct a comparative analysis of gradient-boosted decision trees, feedforward artificial neural networks (ANN), and recurrent neural networks (RNN) for ETA prediction in IWT. Their results show that RNNs achieve the highest prediction accuracy among the tested models. However, the study does not incorporate real-time traffic conditions or environmental factors specific to inland navigation. El Mekkaoui et al. (2023) develop a deep learning-based approach for VAT prediction that integrates AIS data with weather-related variables to enhance forecasting accuracy. Since 2023, research has increasingly emphasized operational and port contextual factors influencing VAT prediction performance. Zhang et al. (2023) employ AIS-derived variables alongside port operational indicators, such as the number of vessels and active cranes, to predict the impact of port congestion on vessel delays using a random forest (RF) model. Chu et al. (2024) first evaluate the accuracy of vessel-reported ETA and observe that its reliability improves as the actual berthing time approaches. Building on this insight, they use vessel-reported ETA as a key input for VAT prediction, achieving a 20% reduction in MAE compared to the vessel reported ETA records. Chu et al. (2025, 2026) propose an innovative data fusion approach that integrates vessel-reported ETAs from port call records with AIS data for VAT prediction. Their method achieves a 55% reduction in MAE, decreasing from 6.84 to 3.11 h, and a 50% reduction in RMSE, from 10.61 to 5.29 h, compared to using vessel-reported ETAs alone. Building upon the improved VAT prediction performance, the study further proposes a feasible predict-then-optimize two-stage framework, in which the predicted VATs are subsequently incorporated into the berth allocation problem to support more efficient berth scheduling decisions.

In the context of IWT, Dobrkovic et al. (2016) pioneer the application of data mining techniques by introducing a novel algorithm for trip segmentation and turn point detection, applicable to both oceanic and inland navigation. This foundational work lays the groundwork for subsequent research on VAT prediction in IWT. Five years later, Noman et al. (2021) conduct a large-scale study using 16 million AIS records from 2395 container vessels operating along the German inland waterway from Bremerhaven to Braunschweig. Using a 70/30 train–test split, their GRU-based model achieves strong performance, with an RMSE of 13.21 min and an MAE of 5.92 min. Fan et al. (2023) analyze AIS data collected over a two-month period from the Yangtze River, proposing a contextualized spatial–temporal model tailored to different vessel types. While their approach highlights variations in travel time prediction across ship categories, it does not incorporate external factors such as weather conditions or river hydrodynamics, which are known to significantly affect navigation and operational efficiency. Wenzel et al. (2023) propose a neural network-based approach for ETA prediction using three months of AIS data. Their method integrates trajectory segmentation with A* algorithm-based distance estimation but considers only AIS-derived features, excluding other contextual factors. In a cutting-edge study, Lei et al. (2024) propose a novel approach to VAT prediction in inland waterways by incorporating traffic flow, which is defined as the number of vessels passing through a given point per unit time, into a tree-based stacking model. As the first to introduce traffic flow as a predictive feature, their method significantly enhances accuracy, achieving precision rates of 90.5% for downstream and 88.6% for upstream vessels. The following Table 1 offers an overview of the related VAT prediction literature review.

2.3. Research gap

Despite significant advances in the field of VAT prediction, several critical gaps remain unaddressed. From a scenario perspective, previous studies have focused primarily on oceangoing vessels, with comparatively limited attention given to IWT. Unlike ocean-going navigation, IWT is characterized by more complex operational environments, winding and narrow routes, and significantly higher vessel traffic density. These factors contribute to increased interactions among vessels and greater variability in travel times, posing unique challenges for accurate VAT prediction. However, existing studies on IWT VAT prediction often fail to reflect these distinctive characteristics and typically adopt methodologies designed for ocean shipping without appropriate contextual adaptation. Moreover, most existing research, whether for inland or ocean-going vessels and particularly those utilizing AIS data, has concentrated mainly on short-distance forecasts, such as predicting the VAT for the final 30 km to a port or destination. However, these short-distance forecasts are not the primary concern of port authorities for daily operations, as they require long-distance predictions to plan berth allocations and other port activities efficiently. From a data perspective, prior studies have predominantly relied on either static ETA reports or dynamic AIS data, with limited integration of both sources (Jiang et al., 2025). In addition, empirical characteristics unique to IWT are rarely considered. Notably, existing AIS-based VAT prediction models often estimate the remaining sailing distance using great-circle approximations, which fail to capture the structural complexity and curvature of inland routes, thereby limiting prediction accuracy in IWT contexts. To bridge these gaps, this study leverages AIS data from European inland vessels and introduces a comprehensive feature set comprising vessel physical attributes, reported ETAs, and meteorological information. The proposed model further incorporates IWT characteristics by explicitly modeling real-time traffic flows and accurately estimating route distances based on the structured topology of navigation networks.

3. Data preprocessing

Data preprocessing involves converting raw AIS data and supplementary datasets into a structured and enriched set of features tailored for VAT prediction. The flowchart of the data preprocessing steps are shown in Fig. 2:

This section begins by outlining the characteristics of IWT and providing background on the Port of Rotterdam, which serves as the case study. The preprocessing process begins with the cleaning and segmentation of raw AIS data into distinct voyage legs, enabling a quantitative assessment of vessel arrival punctuality. The inland waterway network is subsequently partitioned into square grid cells with a side length of 1 km; for each node, traffic flow is computed, and the remaining travel distance for each vessel is estimated using the A* algorithm. Finally, data fusion and feature engineering are applied to integrate and refine a comprehensive set of features, thereby supporting more accurate VAT predictions.

Table 1
Results of the analysis of articles published for ETA prediction in the maritime sector.

Reference	Focus		Methods		Algorithm	Data used
	IV	OV	PF-VAT	DE-VAT		
Dobrkovic et al. (2016)	√			√	GA	AIS
Kim et al. (2017)		√		√	DT, KNN, LR	AIS
Last et al. (2019)		√	√		Not applicable	AIS
Wu et al. (2020)		√		√	IIM	AIS
Štepec et al. (2020)		√		√	Catboost	AIS, port
Viellechner and Spinler (2020)		√		√	NN, RF, SVM	AIS
Ogura et al. (2021)		√	√		Bayesian learning	AIS, weather
Park et al. (2021)[a]		√	√		Bayesian learning	AIS
Noman et al. (2021)[a]		√	√		GBDT, FANN, RNN	AIS
Xu et al. (2022)		√	√		Regression model	AIS
El Mekkaoui et al. (2023)		√		√	MLP, LSTM, CNN, Wavenet	AIS, weather
Zhang et al. (2024)		√		√	XGBoost, SHAP	AIS, port
Fan et al. (2023)[a]		√		√	CNN, LSTM	AIS
Kim et al. (2023)		√	√		Gradient dropout	AIS
Wenzel et al. (2023)	√			√	NN	AIS data
Zhang et al. (2024)		√	√		TCN	AIS
Lei et al. (2024)	√	√		√	XGBoost	AIS, weather, river
This study	√			√	XGBoost, LightGBM, LSTM	AIS, ETA weather, traffic flow

Focus: IV (Inland vessels), OV (Ocean-going Vessels).
Methods used: PF-VAT (Reconstructing vessel trajectories and applying path-finding algorithms to estimate VAT), DE-VAT (data engineering, where VAT is directly predicted by extracting features from the vessel's navigation data).
Algorithms: DT (Decision Tree), KNN (K-nearest Neighbors), LR (Linear Regression), TCN (Temporal Convolutional Network) Data: AIS (Automated Identification System), LRIT (Long Range Identification and Tracking), CNN (Convolutional Neural Network), NN (Neural Network), RF (Random Forest), SVM (Support Vector Machine), GBDT (Gradient Boosting Decision Trees), MLP (Multi-Layer Perceptron Neural Network), GRU (Gated Recurrent Unit Neural Network), LSTM (Long Short-Term Memory), SHAP (SHapley Additive exPlanations), GA (Genetic Algorithm), IIM (Iterative Interpolation-Based Method).
[a] These studies predict the trajectory of individual vessels to estimate accurate short-distance VAT, which significantly differs from the approach of this study, where VAT is directly predicted for multiple inland vessels using data engineering methods (DE-VAT).

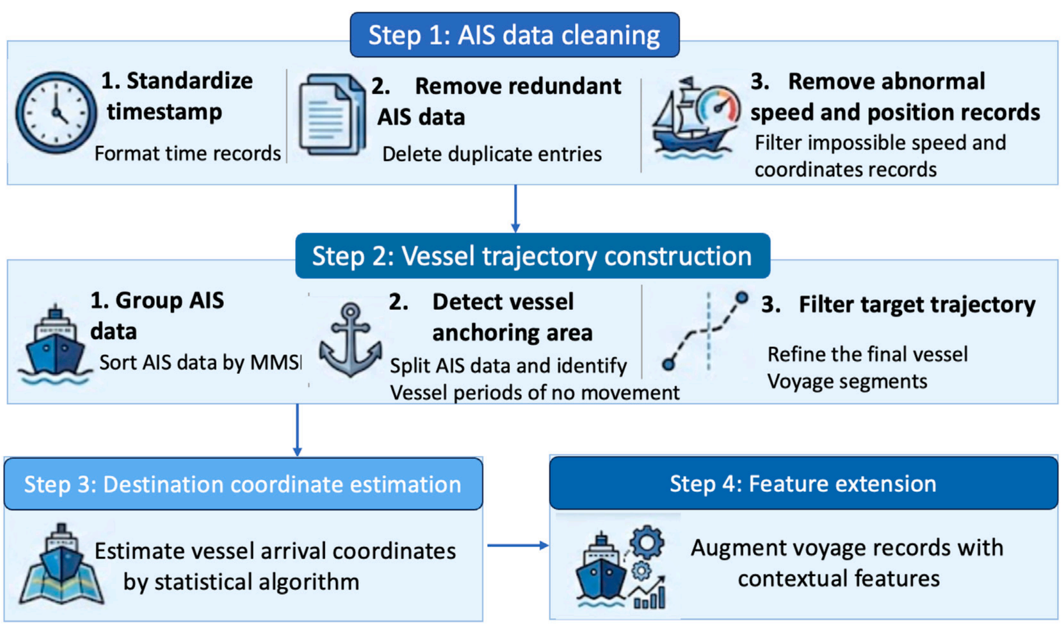

Fig. 2. Workflow of the data preprocessing.

3.1. Introduction to Port of Rotterdam

This study centers on the Port of Rotterdam, one of Europe's largest and busiest ports, handling approximately 438 million tonnes of cargo annually (Havenbedrijf Rotterdam B.V., 2023). Each year, the port accommodates around 28,000 sea-going vessels and 90,000 inland barges. Efficient terminal operations for inland vessels heavily rely on accurate ETA. For this analysis, AIS data for inland waterway vessels en route to the Port of Rotterdam in Europe, covering the period from January 1st, 2022 to March 31st, 2022, are utilized.

Fig. 3 illustrates the layout and dimensions of terminal facilities at the Port of Rotterdam. Terminals at the port are generally equipped with separate berths for inland barges and sea-going vessels to accommodate their distinct operational needs. In Fig. 3, the solid-lined rectangle marks the area designated for IWT vessels operations, while the dotted area represents berths for sea-going ships. This infrastructure enables the Port of Rotterdam to plan and manage IWT operations independently, enhancing the efficiency and reliability of inland vessel scheduling and resource deployment. Fig. 4 presents a heatmap visualizing vessel movements en route to the Port of Rotterdam. The multiple routes taken towards the port highlight the complexity and spatial variability of inland waterway traffic patterns, reflecting the intricate dynamics of IWT and underscoring the importance of accurate VAT predictions.

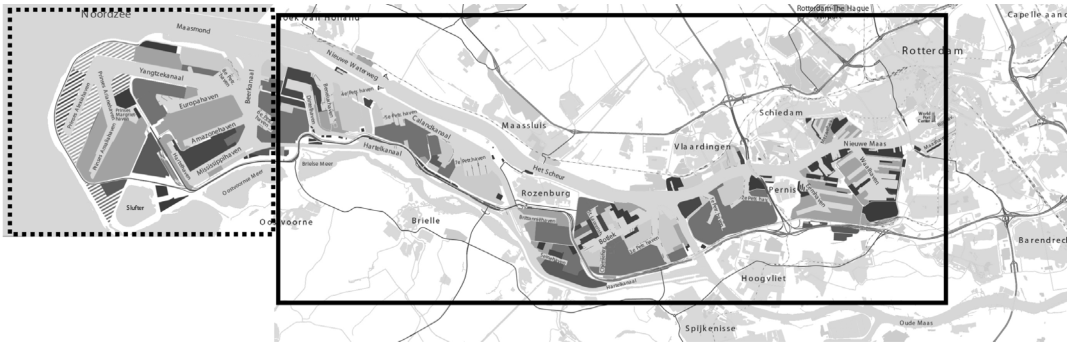

Fig. 3. Map of terminals in the Port of Rotterdam.

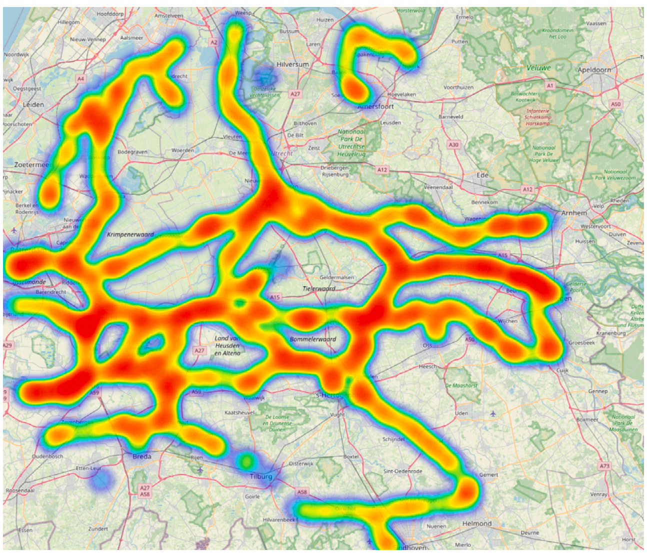

Fig. 4. Heatmap of barges traveling to the Port of Rotterdam.

3.2. Data cleaning

The data cleaning procedure ensures that the trajectories of each vessel's journey can be distinctly identified within the original AIS dataset, thereby providing a solid foundation for subsequent analysis. This process consists of two main steps: AIS data cleaning and vessel trajectory construction.

3.2.1. AIS data cleaning

The longitude and latitude of vessels, key components of AIS data, often contain positional inaccuracies and occasional gaps. To address this, the AIS data cleaning process focuses on correcting dynamic positioning data derived from AIS reports. A thorough statistical analysis has identified three primary error types in the dataset: irregular track positions, anomalous speeds, and inconsistent trajectory directions (Lei et al., 2024). Based on these findings, the following AIS data leaning rules have been established:

(1) Standardizing the timestamp format is crucial, as discrepancies may arise in how timestamps are recorded. The standardized format for AIS timestamps is "YYYY-MM-DD HH:MM:SS" Entries with missing or incomplete timestamps are excluded to ensure data consistency.
(2) Removing redundant AIS records is essential for data reliability. Redundancies often occur when a vessel is stationary and records are repeatedly logged. To address this, if the speed at the ith record exceeds 1 knot while the position remains the same as at the (ith $-$ 1) record, the redundant entry is discarded.
(3) Records with abnormal speeds are filtered out. Inland vessels typically do not exceed 14 knots; therefore, AIS records showing speeds above 14 knots are considered outliers and removed.
(4) Significant deviations of a vessel's position from its expected trajectory can distort the average speed and degrade overall data accuracy; therefore, records exhibiting such substantial positional offsets are removed from the dataset.

The AIS dataset initially contains 200,791,038 records covering the period from January 1st 2022 to March 31st, 2022. After applying the data cleaning procedures, the number of records reduces to 149,797,113. Although abnormal data have been removed, the AIS dataset still consists of mixed records without segmentation into individual voyages. Moreover, within the given period, the same vessel may call at the Port of Rotterdam multiple times, and the dataset also includes trajectories of vessels that transit through the waterways without docking at the port. Therefore, further vessel trajectory construction is required to delineate individual voyages and isolate AIS data specific to vessels calling at the Port of Rotterdam.

3.2.2. Vessel trajectory construction

To extract the specific voyage data for each vessel, the Maritime Mobile Service Identity (MMSI) number, which serves as a unique identifier for each ship, is utilized. This enables the filtering of the relevant AIS records from the dataset, thereby facilitating the construction of the voyage trajectory for each vessel. The detailed steps involved in the construction of the vessel trajectory are outlined as follows:

1. Grouping the AIS data: AIS records for each vessel are grouped using the MMSI number as a unique identifier. These records may include trajectory data from multiple voyages over a given period.
2. Identifying Cutting Points: The grouped trajectories are segmented into individual voyages based on temporal discontinuities, by analyzing the time intervals between consecutive AIS records and identifying a cutting point whenever the gap exceeds 2 h (Lei et al., 2024).
3. Detecting Stay Points: Stay points are identified within each segmented trajectory by locating a sequence of at least 10 consecutive AIS records whose coordinates remain within a confined spatial area, defined as a radius of 500 m, for a duration of at least 30 min. Such segments are regarded as stay points, indicating anchoring or port stay events.
4. Filtering Target Trajectories: Finally, the processed trajectories are filtered to retain only those voyages whose endpoints lie within the Port of Rotterdam area, ensuring the relevance of the constructed trajectories to the study objectives.

After processing and segmenting the voyages, a total of 6,446,265 AIS data points remain, corresponding to 4192 constructed trajectories. Each AIS data point includes an ETA reported by the vessel, whereas the

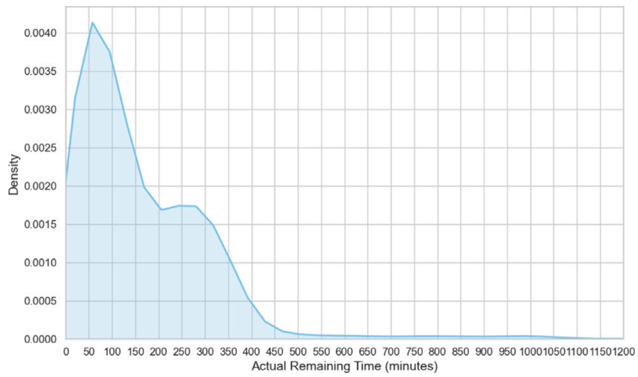

Fig. 5. Density analysis of actual remaining time for each AIS record.

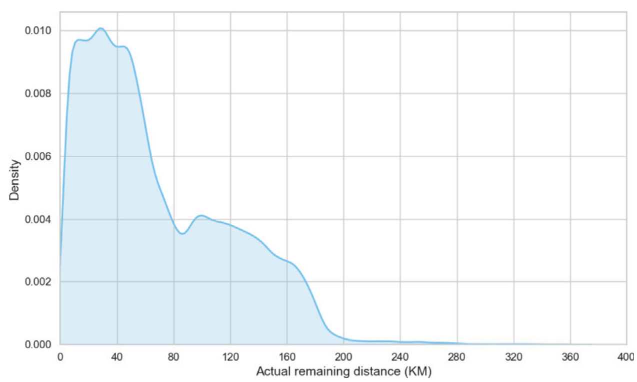

Fig. 6. Density analysis of actual remaining distance for each AIS record.

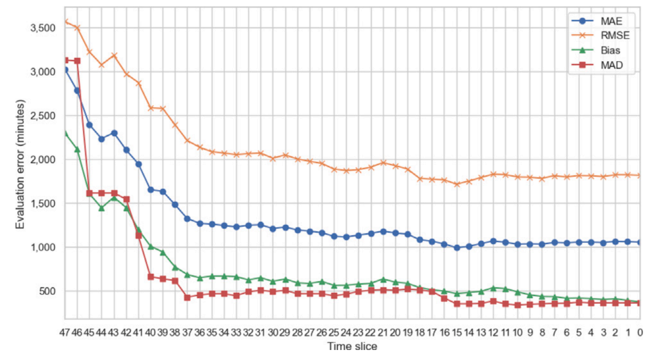

Fig. 7. Evaluate the ETA accuracy in different time slices.

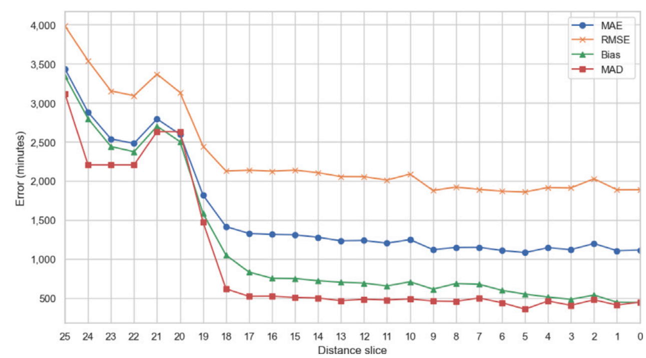

Fig. 8. Evaluate the ETA accuracy in different distance slices.

original data and port call records do not directly provide the ATA for each trajectory. Therefore, the ATA needs to be manually constructed based on the observed AIS trajectory. In this study, the timestamp of the last AIS point within the port area in each trajectory is used as an approximation of the vessel's ATA.

3.3. Vessel arrival analysis at the port of Rotterdam

Before conducting VAT prediction, a quantitative analysis of the AIS dataset is performed. As an initial step, the actual remaining travel time and distance for each AIS record are calculated. Specifically, the remaining travel time is obtained by subtracting the AIS report time from the vessel's ATA, while the remaining distance is computed incrementally by summing the distances from each AIS point to the destination, starting from the second-to-last point. Visualizations of the actual remaining travel time and distance are presented in Figs. 5 and 6, respectively. Fig. 5 shows that the actual remaining travel time for the majority (95.1% of the data) of AIS data is within 450 min, while Fig. 6 indicates that the actual remaining traveling distance for most AIS data (99.5% of the data) is within 250 km.

Subsequently, the punctuality of vessel arrivals at the Port of Rotterdam is evaluated and analyzed. The punctuality of arrival of the vessel is defined as the discrepancy between the ETA reported by the vessel and the corresponding ATA. However, directly comparing ETA data recorded at different temporal and spatial proximities to arrival is not meaningful. For example, an ETA record reported 10 min and 1 km before arrival is generally far more accurate than an ETA reported 10 h and 100 km in advance, rendering direct comparisons invalid. To address this issue, the AIS data are segmented into distinct time and distance intervals before conducting any comparative analysis.

To fairly evaluate vessel-reported ETA punctuality in both spatial and temporal dimensions, the AIS data are discretized into time slices, based on actual remaining travel time, from "0 min" to "≥450 mins" in 10-minute intervals (46 slices), and into distance slices, based on actual remaining travel distance, from "0 dis_slice" to "≥25 dis_slice" in 10-kilometer intervals (26 slices), for subsequent analysis.

The "0 mins" time slice includes AIS data records where the time difference between the AIS report time and its corresponding ATA ranges from 0 to 10 min. The "≥450 mins" time slice encompasses AIS data records where the time difference is at least 450 min (e.g., 450 or 500 min). Similarly, the "0 dis_slice" distance slice includes AIS data whose actual remaining traveling distance is between 0 and 10 km. The "≥250 dis_slice" includes AIS data records where the remaining traveling distance is at least 250 km.

Four metrics are used to evaluate the accuracy of the vessel-reported ETA, with the ATA serving as the ground truth and the reported ETA or model prediction as the estimated value. These metrics include RMSE, MAD, bias, and MAE, and are defined as follows. Given a total of n AIS records, where y_i represents the ATA and $\hat{y}_i$ represents the ETA for vessel AIS record i, with $i = 1, \dots, n$:

RMSE:

$$RMSE = \sqrt{\sum_{i=1}^{n} \frac{\left(\hat{y}_i - y_i\right)^2}{n}}. \tag{1}$$

MAD:

$$\mathrm{MAD} = \frac{\sum_{i=1}^{n} \left|y_i - \bar{y}\right|}{n}. \tag{2}$$

Bias:

$$\mathrm{Bias} = \frac{\sum_{i=1}^{n} (y_i - \hat{y}_i)}{n}. \tag{3}$$

MAE:

$$\mathrm{MAE} = \frac{1}{n} \sum_{i=1}^{n} \left|y_i - \hat{y}_i\right|. \tag{4}$$

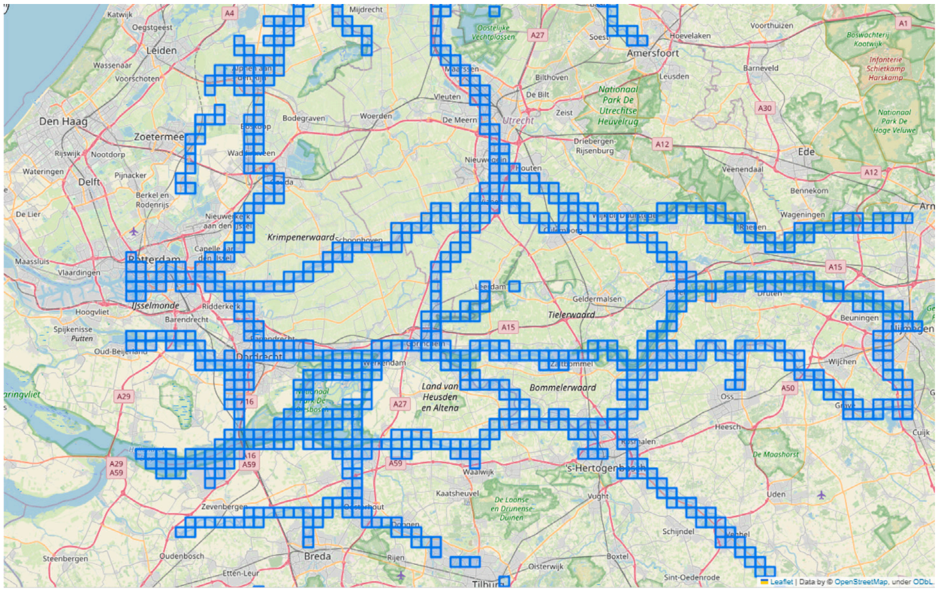

Fig. 9. Detailed view of the river segments to the port of Rotterdam.

The evaluation results for vessel arrival punctuality across different time and distance slices are presented in Figs. 7 and 8. In both Figures, the vertical axis represents the error metrics measured in minutes, while the horizontal axis denotes the respective time or distance slices. As shown in Fig. 7, the accuracy of vessel-reported ETA data increases as the time difference between the report and the actual arrival decreases. Similarly, Fig. 8 demonstrates that ETA accuracy improves as the vessel's distance to its destination reduces. This trend is consistent across all evaluation metrics, indicating that overall errors decrease as vessels approach the port, both temporally and spatially. However, it is noteworthy that despite this improvement, the average ETA error remains approximately 500 min even when vessels are near the port. This substantial error margin highlights that relying solely on vessel-reported ETA data for berth planning is unreliable and may lead to significant operational issues.

3.4. Inland waterway segmentation

Compared to ocean shipping, inland shipping operates on fixed and well-defined waterways, providing more stable and predictable routes unaffected by ocean tides (Lei et al., 2024). Its dense network extends deep into inland regions, and the shorter travel distances make it particularly suitable for efficient regional freight transportation. In the context of ocean shipping research, vessel travel distances are typically calculated using straight-line or great-circle formulas derived from the latitude and longitude of departure and arrival points. However, this method yields unreliable results for IWT, as the meandering courses of rivers prevent vessels from following direct trajectories between two locations. To improve the accuracy of IWT vessel voyage distance estimation, the IWT network is first divided into segments represented by nodes within square grids of 1 km radius, with nodes that do not contain any AIS vessel trajectories subsequently removed. The following Fig. 9 shows the segments created based on the waterways in the Netherlands. Following the segmentation of inland waterways, the A* algorithm is employed to evaluate the remaining sailing distance for vessels. A* algorithm is a widely recognized heuristic search algorithm for pathfinding and graph traversal, combining the thoroughness of Dijkstra's algorithm with the efficiency of greedy search, thereby ensuring optimal path discovery while reducing computational overhead (Hart et al., 1968; T.-Y. Yang et al., 2025). In this context, the A* algorithm is utilized to generate an approximated remaining sailing path on the discretized waterway network. The distance between the vessel's current position and the centroid of the next node along this path is then computed, and these distances are incrementally summed to estimate the vessel's remaining travel distance. Furthermore, the segmented nodes facilitate the analysis and monitoring of vessel traffic flow within each node region, offering valuable insights into localized traffic patterns.

3.5. Destination coordinate estimation

When predicting VAT, some studies regard the last recorded AIS position of a vessel as its destination. However, this approach is not suitable for a real prediction setting, because the exact final stopping position is posterior information that is unavailable before the vessel arrives. In practical port operations, the definition of arrival may also depend on berth availability and port operating rules. If a berth is available, a vessel may be regarded as having arrived when it reaches the berth; if the berth is occupied, arrival may instead be recorded when the vessel reaches an anchorage or designated waiting area. Such operational ATA information is usually recorded by port staff in port call records. Since the dataset used in this study only contains AIS records and does not provide official ATA records, a representative destination point needs to be inferred from historical AIS trajectories for remaining-distance estimation.

Specifically, the latitude and longitude of the last AIS point in each voyage trajectory are first extracted from the AIS dataset. The mean latitude and longitude of these endpoints are then calculated to establish a central reference point. Following the data-processing approach of Chu et al. (2025), the 90th percentile of the final coordinates closest to this reference point is selected, and their average is used as the estimated destination point. This estimated point is not intended to represent a universal official arrival location; rather, it provides a consistent data-driven reference for calculating the vessel's remaining voyage distance during VAT prediction. Fig. 10 illustrates the distribution of voyage endpoints from historical AIS data, while Fig. 11 shows the estimated destination point after processing. The influence of alternative destination-point selection methods is further evaluated through the sensitivity analysis presented in Section 4.

3.6. Feature extension

This subsection aims to construct a comprehensive feature set for VAT prediction based on the foundational AIS dataset. Specifically, AIS

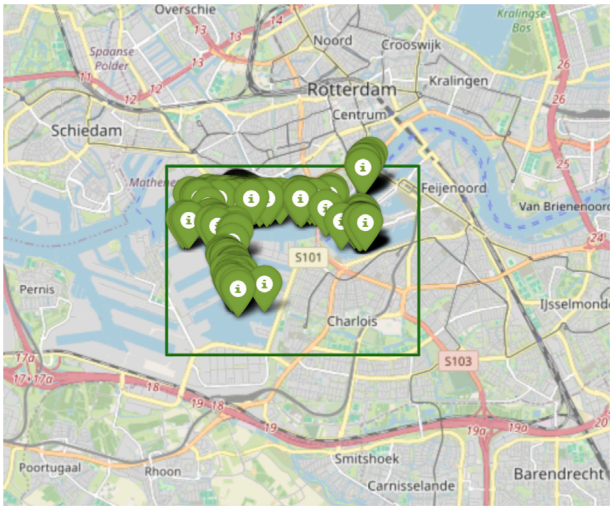

Fig. 10. The collection of endpoint coordinates.

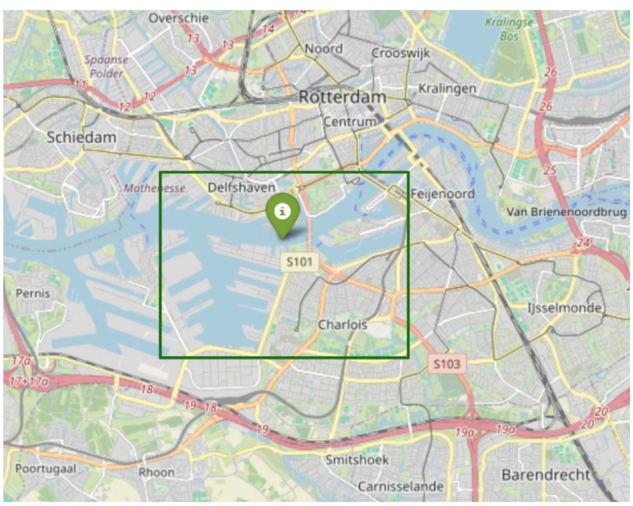

Fig. 11. A schematic diagram of the estimated destination point.

dynamic data are first used as the primary data source, and are then complemented with additional information from vessel physical characteristics, port call records, and environmental observations. Based on this multi-source data foundation, further feature mining is conducted to derive a richer set of predictive variables. As a result, five categories of features are ultimately considered for VAT prediction, including vessel physical features, spatial features, temporal features, traffic-related features, and environmental and waterway features. To facilitate model learning, the prediction target is not directly defined as VAT itself, which is an absolute timestamp, but as the vessel's remaining voyage time at each AIS observation point. In this way, the predicted VAT can be recovered by adding the model output to the corresponding AIS report time. Therefore, the ground-truth target is computed as the time interval between the ATA and the AIS report timestamp. Detailed descriptions of the constructed features are provided below.

Vessel physical features are integrated into the AIS-based dataset by using the *Call_sign* in each AIS record to match the corresponding vessel profile information from the external vessel database. This step enriches the original dynamic AIS observations with static vessel-specific attributes that are relevant to VAT prediction. Specifically, vessel length and width are included to describe the vessel's dimensions, gross tonnage is used to reflect its cargo-carrying capacity, and vessel type is considered because different vessel categories may follow different sailing, docking, and operational patterns (Chu et al., 2024). These attributes are closely related to maneuverability, berthing requirements, and possible waiting time, and therefore play an important role in VAT prediction. Incorporating them allows the model to consider both the intrinsic properties of the vessel and the external logistical constraints it may face, thereby improving the predictive accuracy and robustness of the proposed framework.

Next, two spatial features are derived based on the AIS data and the estimated destination point from the previous subsection. The first feature, denoted as "Exp_directdistance", is the estimated remaining voyage distance calculated as the great-circle distance from each AIS point to the estimated destination using the Haversine formula (Chu et al., 2025). The second feature, denoted as "Exp_astardistance", is the estimated remaining voyage distance calculated using the A* algorithm, which determines the shortest distances between adjacent nodes and then sums these distances along the navigable path from the current AIS point to the destination. These spatial features capture both the shortest direct distance and the vessel actual navigable route, reflecting the characteristics of IWT and providing valuable information to enhance the accuracy of VAT prediction.

Next, four time-related features are considered to enhance VAT prediction. The first is the vessel's instantaneous speed reported in the AIS data. Based on this information, three additional temporal features are constructed to characterize the vessel's remaining voyage time from different perspectives: (i) the estimated remaining time obtained by dividing the great-circle distance to the destination by the current vessel speed, (ii) the estimated remaining time obtained by dividing the network-based remaining sailing distance calculated by the A* algorithm by the current vessel speed, and (iii) the time difference between the vessel's reported ETA and the AIS report timestamp. It should be noted that ETA is an important port call-related variable in this study. For AIS records in which ETA is directly available, the reported value is used directly. Otherwise, ETA information is fused into the AIS dataset through temporal matching within the same vessel. Specifically, for each vessel identified by its call sign, let $\mathcal{A}_v = \{a_1, \dots, a_m\}$ denote the chronologically ordered AIS records with report times $t_1^{AIS} \le \cdots \le t_m^{AIS}$, and let $\mathcal{E}_v = \{e_1, \dots, e_n\}$ denote the chronologically ordered ETA reports with report times $t_1^{ETA} \le \cdots \le t_n^{ETA}$. For each AIS record a_i, the matched ETA is defined as the most recent ETA report issued no later than the AIS report time, namely

$$e^*(a_i) = \arg\max_{e_j \in \mathcal{E}_v} \left\{ t_j^{ETA} \mid t_j^{ETA} \le t_i^{AIS} \right\}. \tag{5}$$

The corresponding ETA value is then assigned to a_i. If no such e_j exists, the AIS record is regarded as unmatched and excluded from subsequent analysis. Based on the matched ETA, the ETA-based remaining time feature is calculated as

$$T_i^{ETA} = ETA_i - t_i^{AIS}. \tag{6}$$

In this way, the temporal feature set incorporates both instantaneous navigation status and voyage-plan-related time information, providing complementary descriptions of the vessel's remaining voyage and improving the model's ability to predict VAT.

The environmental features considered in this study include temperature, river speed, and wind speed. Temperature reflects the ambient weather condition in the Port of Rotterdam, while river speed and wind speed are matched to each AIS record according to the vessel's spatiotemporal location. Specifically, for each AIS record, the nearest meteorological station is identified based on the geographic distance between the vessel location and all candidate stations. The distance is calculated using the latitude and longitude coordinates through the Haversine formula:

$$d = 2R \arcsin\left(\sqrt{\sin^2\left(\frac{\phi_2 - \phi_1}{2}\right) + \cos(\phi_1)\cos(\phi_2)\sin^2\left(\frac{\lambda_2 - \lambda_1}{2}\right)} \right), \tag{7}$$

Table 2
Feature description for VAT prediction.

Feature category	Feature	Description	Data source
Vessel physical features	Length Width Gross tonnage	Vessel length from bow to stern Maximum vessel width Total internal volume capacity	MMSI records matching
	Type	Vessel classification	One-hot encoded
Spatial features	Exp_directdistance Exp_astardistance	Straight-line remaining distance to destination Remaining distance via A* algorithm routing	AIS data estimation
Temporal features	Exp_aistime Exp_astartime Speed	Estimated time based on AIS distance and current speed Estimated time based on A* distance and current speed Real-time vessel speed from AIS	Calculated from AIS data
	Exp_etatime	Reported ETA minus current time	ETA records
Environmental features	Temperature River speed Wind speed	Ambient temperature at Rotterdam port Current velocity in vessel vicinity Current wind speed in vessel vicinity	Meteorological stations
Waterway features	Trafficflow Node number	Vessel count in port area at reporting time Number of routing nodes in remaining path	A* algorithm computation
	Water level	Current water surface elevation	Meteorological stations
Target variable	Actual_remaining_time	Ground truth voyage completion time	ATA minus AIS timestamp

where d denotes the great-circle distance between the vessel and a meteorological station, R is the radius of the Earth, ϕ_1 and ϕ_2 are the latitudes of the vessel and the station, λ_1 and λ_2 are their longitudes. After identifying the nearest station, the environmental observation with the closest timestamp later than the AIS record time is selected for matching, so as to maintain temporal consistency between navigation status and environmental conditions. In this way, each AIS observation is enriched with localized environmental information, allowing the model to better capture the effect of surrounding operating conditions on vessel arrival behavior.

Finally, three innovative waterway features are introduced: vessel traffic flow, the number of nodes traversed by the vessel, and the real-time water depth at the vessel's AIS-reported location, which have not been considered in previous VAT prediction studies and are explained in detail below.

Vessel traffic flow refers to the number of vessels passing through a specific area within a given time frame. This feature plays a crucial role in determining the VAT in IWT, as it directly affects navigation efficiency and congestion levels (Lei et al., 2024; Zhang et al., 2025a). High traffic density can result in delays due to limited channel capacity, longer waiting times at locks, and an increased risk of traffic conflicts, particularly in narrow or heavily trafficked sections. In contrast, smooth traffic flow facilitated by effective scheduling and real-time traffic management reduces delays and improves the predictability of VAT. Compared to ocean-going navigation, IWT features more defined and restricted routes, making it easier to accurately assess traffic flow conditions (Lei et al., 2024). In this study, traffic flow data from the past 10, 20, and 30 min are analyzed for the nodes in which vessels are located at the time of reporting AIS data, with each node defined as a square area with a radius of 1 km. The corresponding traffic flow features are denoted as `traffic_10_min`, `traffic_20_min`, and `traffic_30_min`, respectively.

The number of nodes refers to the total number of nodes that the vessel will pass through along its remaining route, reflecting the remaining travel distance and potentially influencing VAT. A longer route with more nodes could indicate a longer remaining travel time, which would affect the ETA. Water levels significantly affect VAT by altering navigability. High water levels deepen channels and generally reduce VAT, while excessively high levels can create strong currents that cause delays. Low water levels restrict channel depth, requiring vessels to reduce speed or load, thus increasing VAT. Fluctuating water levels also impact lock and port operation efficiency, further influencing arrival times. The features used to predict VAT, along with the ground truth values and prediction target, are summarized in Table 2.

4. Experiments

This section first introduces the models used for VAT prediction and implements them on the integrated dataset to forecast VAT. This is followed by a comprehensive quantitative analysis of the prediction results, including feature importance analysis based on model outputs and SHAP values. Finally, the section discusses the insights gained from VAT prediction and their implications for real-world port operations.

4.1. Prediction model introduction

In this study, the integrated AIS dataset is structured as tabular data, where each row corresponds to an observation or target value and each column represents a feature, a common format in transportation research (Filom et al., 2022). Tree-based algorithms, such as RF and XGBoost, often outperform neural networks on tabular datasets due to their efficient feature extraction and ensemble learning capabilities (Grinsztajn et al., 2022; Xiong et al., 2025). Using these strengths, tree-based models are developed for VAT prediction using the pre-processed AIS dataset, with each row used to predict a corresponding VAT value. In addition, state-of-the-art neural networks are applied to benchmark their performance against tree-based models.

RF is an ensemble learning method that enhances decision tree performance for classification and regression tasks. It builds multiple trees using bootstrapped samples of the training data and random subsets of features, introducing diversity that reduces overfitting and improves generalization (Zhou, 2021; Zhang et al., 2025b). For regression tasks, the RF prediction is computed as the average of the individual tree predictions:

$$\hat{y} = \frac{1}{T} \sum_{t=1}^{T} \hat{y}_t, \tag{8}$$

where T is the total number of trees, and $\hat{y}_t$ is the prediction from the tth tree. This averaging process smooths out individual tree errors and mitigates the impact of noise in the data, leading to more accurate and reliable predictions compared to a single decision tree. A key advantage of the RF and other tree-based models is its ability to evaluate the importance of the characteristics. This is achieved by measuring the decrease in impurity (e.g., Gini impurity or mean squared error) across all trees whenever a feature is used to split the data. The feature importance score is typically calculated as:

$$F_j = \frac{1}{T} \sum_{t=1}^{T} \Delta I_{j,t}, \tag{9}$$

where $\Delta I_{j,t}$ represents the reduction in impurity for feature j in tree t. This capability provides insights into which features contribute most to the model's predictions, offering an interpretative layer to RF and making it a powerful tool for exploratory data analysis and feature selection. In general, RF leverages its ensemble structure and inherent randomness to deliver robust and interpretable results, making it widely applicable across various domains.

XGBoost is an efficient implementation of gradient boosting that builds a strong predictive model by sequentially adding weak learners, typically decision trees. The key idea is to minimize a specified loss function L by iteratively improving the model's predictions (Chen and Guestrin, 2016). At each iteration t, a new tree $h_t(x)$ is added to correct the residuals of the previous model. The updated model prediction $\hat{y}_i^{(t)}$ for each data point i is expressed as:

$$\hat{y}_i^{(t)} = \hat{y}_i^{(t-1)} + \eta h_t\left(x_i\right), \tag{10}$$

where η is the learning rate. The objective function $\mathcal{O}$ is includes a loss term and a regularization term to prevent overfitting:

$$\mathcal{O} = \sum_{i=1}^{n} L\left(y_i, \hat{y}_i^{(t)}\right) + \sum_{t=1}^{T} \Omega\left(h_t\right). \tag{11}$$

The regularization term $\Omega\left(h_t\right)$ ensures model simplicity and is defined as:

$$\Omega\left(h_t\right) = \gamma T + \frac{1}{2}\lambda \sum_{j=1}^{T} w_j^2, \tag{12}$$

where T is the number of leaves in the tree, w_j is the weight of the jth leaf, and γ, λ are regularization parameters. By optimizing objective function $\mathcal{O}$ XGBoost achieves high accuracy, robustness, and prevents overfitting.

LightGBM is an efficient and scalable implementation of the GBDT algorithm (Ke et al., 2017). It is designed to handle large-scale datasets and high-dimensional features while maintaining high accuracy and efficiency. Compared to traditional GBDT implementations, such as XGBoost, LightGBM introduces several optimizations, including histogram-based decision tree learning, leaf-wise tree growth, and efficient memory usage, which significantly accelerate training and reduce resource consumption. LightGBM uses the gradient boosting framework to iteratively minimize a loss function $L(y, \hat{y})$, where y represents the true target values and $\hat{y}$ represents the predicted values. The model starts with an initial constant prediction:

$$\hat{y}^{(0)} = \arg\min_{c} \sum_{i=1}^{n} L\left(y_i, c\right), \tag{13}$$

and then improves the predictions iteratively. At each iteration t, it fits a decision tree $f_t(x)$ to the negative gradient of the loss function:

$$g_i^{(t)} = -\frac{\partial L\left(y_i, \hat{y}_i^{(t-1)}\right)}{\partial \hat{y}_i^{(t-1)}}, \tag{14}$$

and updates the predictions as follows:

$$\hat{y}_i^{(t)} = \hat{y}_i^{(t-1)} + \eta f_t\left(x_i\right), \tag{15}$$

where η is the learning rate, controlling the contribution of each tree. To improve splitting accuracy, LightGBM uses a second-order Taylor approximation of the loss function:

$$L(y, \hat{y}) \approx L\left(y, \hat{y}^{(t-1)}\right) + g_i^{(t)} \Delta\hat{y} + \frac{1}{2} h_i^{(t)} (\Delta\hat{y})^2 \tag{16}$$

where $h_i^{(t)}$ is the second-order gradient. The best split is chosen by maximizing the information gain:

$$\text{Gain} = \frac{1}{2}\left(\frac{G_L^2}{H_L + \lambda} + \frac{G_R^2}{H_R + \lambda} - \frac{\left(G_L + G_R\right)^2}{H_L + H_R + \lambda}\right) - \gamma, \tag{17}$$

where G_L, G_R are first-order gradients, H_L, H_R are second-order gradients, λ is a regularization parameter, and γ is the penalty for splitting. These features, along with categorical feature support and optimized memory usage, make LightGBM highly efficient and widely used in industrial applications.

Neural networks are a fundamental component of machine learning, widely applied to tasks such as classification, regression, and pattern recognition. Structurally, a typical neural network consists of an input layer, one or more hidden layers, and an output layer. The input layer receives the raw data, the hidden layers transform and extract representations through weighted connections and activation functions, and the output layer generates the final predictions or classifications. During training, the network iteratively adjusts the weights of its connections to minimize the discrepancy between predicted and actual outputs, commonly using optimization algorithms like gradient descent. Among neural network architectures, Recurrent Neural Networks (RNNs) are specifically designed to handle sequential data by maintaining information from previous inputs. However, traditional RNNs often suffer from vanishing or exploding gradient problems when processing long sequences, which severely limits their ability to capture long-term dependencies.

To overcome the limitations of traditional RNNs, Long Short-Term Memory (LSTM) networks were introduced as a special architecture incorporating memory cells to maintain information over long time periods, effectively addressing the vanishing gradient problem. Since AIS data are time series reflecting vessel movements over time, LSTM is suitable for capturing their temporal dependencies. LSTM networks achieve this through three gates: the forget gate, which discards irrelevant information; the input gate, which updates the cell state with new information; and the output gate, which determines the output based on the cell state. In our study, we implement a two-layer LSTM with 128 hidden units per layer, followed by a fully connected layer to produce the final VAT prediction (Zhou, 2021).

4.2. Prediction result

In this subsection, a detailed analysis of VAT prediction results is presented. Since the integrated VAT dataset is constructed from AIS records, which are inherently time-dependent, a standard random split is not suitable for this study. Although a random split may create more balanced training and testing sets in terms of voyage length, arrival time, and environmental conditions, it may also place observations from later periods in the training set while assigning earlier observations to the test set. In this case, future vessel movement patterns, traffic conditions, or environmental information could be unintentionally used to predict earlier samples, leading to potential data leakage and an overly optimistic evaluation. To better reflect the practical VAT prediction scenario, where models are trained using historical AIS records and then applied to future vessel reports, the dataset is split chronologically according to AIS report time. Specifically, the first 80% of the data, corresponding to earlier report times, is used for training, while the remaining 20% is used for testing. For instance, in a one-year dataset, AIS reports from January to August are allocated to the training set, and data from September to December constitute the test set. This chronological split ensures that the model is trained on past data and evaluated on future data, thereby simulating a real-world forecasting scenario. In addition, the hyperparameters of all compared models are tuned using grid search with 5-fold cross-validation on the training set, and the detailed search space and selected parameter settings are provided in Appendix to ensure reproducibility.

To assess the influence of different features, feature ablation is conducted by removing specific feature groups and retraining the model. Four scenarios are designed. The first scenario includes all features, representing normal VAT prediction training. The second scenario excludes the ETA feature, specifically `Exp_etatime`, meaning the expected remaining voyage time estimated from ETA is not considered. This setting highlights the importance of the vessel-reported ETA in VAT prediction.

Table 3
Prediction performance of models on the time-order test dataset.

Model	All variables				All variables except ETA features				All variables except AIS features				All variables except waterway features			
	MAE	RMSE	R^2	MAD	MAE	RMSE	R^2	MAD	MAE	RMSE	R^2	MAD	MAE	RMSE	R^2	MAD
Vessel ETA	17.06	29.99	−0.73	5.20	–	–	–	–	17.06	29.99	−0.73	5.20	17.06	29.99	−0.73	5.20
Estimated time	4.98	14.03	−0.02	2.26	4.98	14.03	−0.02	2.26	–	–	–	–	4.98	14.03	−0.02	2.26
RF	5.20	13.99	0.21	2.33	4.91	13.24	0.41	2.11	5.91	15.95	0.20	3.88	5.51	15.21	0.21	2.91
LightGBM	3.53	**11.03**	**0.61**	**1.41**	4.07	11.48	**0.52**	1.68	4.23	**11.32**	0.60	2.31	3.56	11.01	0.61	1.51
XGBoost	**3.49**	11.04	0.69	1.40	**3.53**	**11.21**	**0.52**	**1.59**	**4.14**	11.92	**0.63**	**1.98**	**3.55**	**10.80**	**0.62**	**1.41**
LSTM	5.33	15.04	0.09	3.00	5.73	15.73	0.33	3.30	6.44	17.23	0.12	4.33	5.48	15.81	0.05	3.21
ANN	7.21	18.19	−0.01	3.33	7.83	18.19	0.03	4.11	8.02	19.15	0.00	5.27	7.51	16.92	−0.05	4.01

The third scenario excludes AIS-related features, namely `Exp_directdistance`, `Exp_astardistance`, `Exp_aistime`, `Exp_astartime`, and `Speed`, meaning AIS-derived parameters are not considered, to highlight the importance of real-time vessel positioning information. The fourth scenario excludes waterway features, specifically `Traffic flow`, `Node number`, and `Water level`, to highlight the importance of waterway conditions for VAT prediction. To provide a comprehensive evaluation of the model's predictive performance, two additional benchmark values are included: the vessel-reported ETA (denoted as Vessel ETA in the table) and the ETA, which is calculated based on the great-circle distance between the current AIS point and the port, representing an industry-standard estimation method. All approaches are evaluated using four metrics: MAE, RMSE, R^2, and MAD. These four metrics are used because they reflect different aspects of prediction performance. MAE captures the average magnitude of prediction errors and is directly interpretable for port operations. RMSE emphasizes large deviations, which are particularly critical in practice because large ETA errors may cause berth planning inefficiencies and operational disruptions. R^2 measures the overall explanatory power of the model, while MAD provides a robust evaluation of error dispersion that is less affected by outliers. Together, these metrics provide a more comprehensive assessment of model accuracy, robustness, and operational usefulness.

Table 3 provides a comprehensive analysis of prediction performance across different models and feature inclusion scenarios for VAT prediction in the time-sliced dataset. The vessel-reported ETA performs poorly, with high errors (MAE: 17.06 h, RMSE: 29.99 h) and a negative R^2 value (−0.73). This negative R^2 indicates that vessel self-reported ETA not only fails to explain the variance in actual arrival times but performs worse than simply using the mean arrival time as a predictor, highlighting its unreliability and potential bias. In contrast, the estimated time, derived from vessel coordinates, speed, and destination distance, achieves significantly better VAT prediction accuracy (MAE: 4.98 h, RMSE: 14.03 h), demonstrating that geometric estimations are far more reliable than self-reported values.

Among the machine learning models, LightGBM and XGBoost consistently outperform other methods. Specifically, XGBoost achieves the lowest MAE (3.49 h) and the highest R^2 value (0.69), indicating it explains nearly 70% of the variance in VAT, while LightGBM achieves the lowest RMSE (11.03 h) and lowest MAD (1.41 h), demonstrating highly accurate and stable predictions with minimal outlier sensitivity. Compared with the simple geometric estimation method, these advanced tree-based models reduce MAE by approximately 30% and RMSE by more than 20%, highlighting the substantial benefits of data-driven learning. RF and LSTM yield moderate performance, with MAE values around 5.2 and 5.33 h, respectively, and relatively low R^2 values (0.21 and 0.09), suggesting limited explanatory power despite acceptable error levels. The ANN model performs the worst among machine learning methods, with MAE (7.21 h) and RMSE (18.19 h) higher than those of RF, LSTM, LightGBM, and XGBoost, and an almost zero R^2, indicating minimal predictive capability for this VAT prediction task. Overall, tree-based gradient boosting models (LightGBM and XGBoost) demonstrate superior performance, achieving both low absolute errors and high variance explanation, making them the most suitable choice for practical VAT prediction deployments.

The feature ablation results in Table 3 provide further insights into the roles of different feature groups in VAT prediction. ETA features provide a direct prior estimate of vessel arrival and therefore serve as an important baseline reference. When ETA features are excluded, the MAE and RMSE of XGBoost remain close to those obtained using all variables, but the R^2 decreases from 0.69 to 0.52. This indicates that AIS-derived movement information and waterway-related features can partly compensate for the absence of ETA in terms of average prediction error, while ETA still contributes useful information for explaining variations in vessel arrival time. AIS features play a more fundamental role because they describe the vessel's observed movement state, including its position, speed, and progress along the voyage. Excluding AIS features causes a clear increase in prediction errors for most models. For example, the MAE of XGBoost increases from 3.49 h to 4.14 h, and the RMSE increases from 11.04 h to 11.92 h. This confirms that real-time vessel movement information is essential for capturing the dynamic evolution of inland vessel trajectories and for updating the predicted remaining sailing time. Waterway features provide supplementary spatial and network context, such as the remaining sailing distance and route-related characteristics. When these features are excluded, the performance of the best-performing models remains relatively stable. For instance, XGBoost achieves an MAE of 3.55 h and an RMSE of 10.80 h. This suggests that waterway features are useful but not dominant, because part of their information may already be reflected in AIS-derived movement patterns and ETA-related information. Overall, Table 3 shows that AIS features are the core source of predictive information, ETA features provide valuable prior arrival information, and waterway features offer additional contextual support. The results also show that XGBoost maintains robust performance across different feature settings.

To further examine the contribution of each data source, we additionally conducted single-source experiments on the time-sliced dataset using only ETA features, only AIS features, or only waterway features. The results in Table 4 show that AIS-only models consistently outperform ETA-only and waterway-only models, indicating that AIS-derived dynamic information provides the strongest standalone predictive signal for VAT prediction. In contrast, waterway-only models perform the worst, suggesting that such contextual information is insufficient when used in isolation. These findings are in line with the feature ablation results above, where removing AIS features causes the largest performance degradation, while removing waterway features has only a marginal impact. More importantly, the full-feature setting still achieves the best overall results, confirming that multi-source integration is beneficial because it combines the dominant contribution of AIS data with the complementary information provided by ETA and waterway-related features.

Table 5 presents the VAT prediction results based on splitting the dataset by vessels' actual remaining sailing distances. The 80% with longer remaining distances are used for training, and the 20% with shorter distances for testing, simulating a practical scenario where models are trained on distant vessels and applied to predict the VAT

Table 4
Prediction performance of models under different input-source settings on the time-order test dataset.

Model	All variables				ETA features only				AIS features only				Waterway features only			
	MAE	RMSE	R^2	MAD	MAE	RMSE	R^2	MAD	MAE	RMSE	R^2	MAD	MAE	RMSE	R^2	MAD
Vessel ETA	17.06	29.99	−0.73	5.20	17.06	29.99	−0.73	5.20	–	–	–	–	–	–	–	–
Estimated time	4.98	14.03	−0.02	2.26	–	–	–	–	4.98	14.03	−0.02	2.26	–	–	–	–
RF	5.20	13.99	0.21	2.33	6.02	15.42	0.10	3.09	5.48	14.41	0.28	2.62	8.26	19.07	−0.06	4.76
LightGBM	3.53	**11.03**	**0.61**	**1.41**	4.88	13.02	0.36	2.05	3.96	**11.61**	0.55	1.71	6.72	16.84	0.01	3.64
XGBoost	**3.49**	11.04	0.69	1.40	**4.76**	12.84	0.39	**1.96**	**3.84**	11.58	**0.57**	**1.63**	**6.55**	**16.37**	**0.03**	**3.41**
LSTM	5.33	15.04	0.09	3.00	6.31	16.58	0.02	3.58	5.71	15.52	0.16	3.19	8.74	19.84	−0.11	5.08
ANN	7.21	18.19	−0.01	3.33	8.11	19.23	−0.06	3.97	7.54	18.41	0.01	3.61	9.63	21.02	−0.15	5.76

Table 5
Prediction performance of models on the distance-order split test dataset.

Model	All variables				All variables except ETA features				All variables except AIS features				All variables except waterway features			
	MAE	RMSE	R^2	MAD	MAE	RMSE	R^2	MAD	MAE	RMSE	R^2	MAD	MAE	RMSE	R^2	MAD
Vessel ETA	22.38	36.70	−0.06	22.28	–	–	–	–	22.38	36.70	−0.06	22.28	22.38	36.70	−0.06	22.28
Estimated time	2.35	10.34	−0.02	4.23	2.35	10.34	−0.02	4.23	–	–	–	–	2.35	10.34	−0.02	4.23
RF	2.01	8.33	0.11	3.83	2.17	9.94	0.32	4.22	4.82	14.17	0.11	9.73	3.11	11.91	0.33	2.75
LightGBM	**1.80**	7.70	0.73	**3.01**	**1.90**	**8.55**	**0.71**	**3.06**	3.52	**10.52**	0.63	2.06	**2.35**	9.54	**0.62**	1.92
XGBoost	**1.80**	**7.65**	**0.75**	3.06	1.91	8.68	0.70	3.66	**3.48**	10.76	**0.66**	**2.03**	2.37	**9.45**	**0.62**	**1.46**
LSTM	1.99	8.71	0.29	4.11	2.10	9.57	0.30	4.00	5.33	15.32	0.23	11.73	3.33	11.99	0.14	2.30
ANN	2.23	10.11	0.05	4.20	2.11	10.11	0.03	4.30	7.22	17.41	0.04	19.02	4.18	12.12	0.09	3.32

of those nearing the port. Compared to the time-sliced results in Table 3, the distance-sliced results in Table 5 further confirm the robustness of tree-based ensemble models under different dataset partitioning strategies. In the distance-based setting, where models are trained on vessels with longer remaining distances and tested on those nearing the port, both LightGBM and XGBoost maintain leading performance. XGBoost again achieves the lowest MAE (1.80 h) and a high R^2 (0.75), while LightGBM records the lowest RMSE (7.60 h) and MAD (3.01 h), indicating consistent predictive accuracy and robustness. Notably, the absolute error metrics under the distance-sliced setting are lower than those in the time-sliced setup, suggesting that using distance as the partitioning variable aligns better with the actual progression of voyages and yields more stable prediction conditions.

Feature ablation under the distance-sliced setting reveals patterns consistent with the time-based analysis: the exclusion of AIS features leads to the most significant performance degradation across all models, particularly for LSTM, whose RMSE increases from 8.71 h to 15.32 h. This underscores the critical role of AIS-derived trajectory and movement data in VAT prediction. Meanwhile, removing ETA features causes only mild accuracy loss for XGBoost and LightGBM, consistent with earlier findings that self-reported ETA contributes limited value. The impact of excluding waterway features remains marginal, suggesting their secondary role in shaping prediction performance. Collectively, these results affirm the conclusion drawn from the time-sliced experiment: AIS features are the most influential, and tree-based models, especially XGBoost, provide the most accurate and reliable VAT predictions across diverse real-world settings.

To further examine the potential impact of centroid-to-centroid routing approximation on distance-based features and downstream VAT prediction, an additional sensitivity analysis is conducted using different spatial resolutions of the waterway network representation. Specifically, the inland waterway network is partitioned into square grid cells with side lengths of 2 km, 1 km, and 500 m, respectively, and the corresponding A* sailing distance and traffic flow features are recalculated under each setting. In addition, a benchmark setting is considered in which the remaining sailing distance is directly calculated based on the centerline between each AIS point and the destination, without incorporating waterway-based route distance or traffic flow features. The corresponding results are reported in Table 3 under the setting of *without waterway features*.

The sensitivity analysis in Table 6 shows that the prediction performance is affected by the spatial resolution of the waterway network representation. In general, the 500 m grid setting achieves slightly better results than the 1 km baseline across most models, while the 2 km grid leads to the weakest performance. This suggests that a finer-grained representation can better capture route geometry and local traffic flow patterns, thereby improving the quality of waterway-related features for VAT prediction. Among all models, XGBoost still delivers the best overall performance under different grid settings. However, the improvement obtained by the 500 m grid remains moderate. From a practical perspective, reducing the grid size from 1 km to 500 m increases the total number of grid cells by approximately four times, which substantially raises the computational cost of route construction, distance estimation, and traffic flow calculation. Given that the present study involves millions of AIS records, the corresponding local experiments become considerably more time-consuming under the 500 m setting.

Moreover, a finer spatial partition does not necessarily eliminate all approximation issues. In some estuary sections of European inland waterways, the navigable width can exceed 500 m. Under the 1 km setting, such a section may still be represented by a single grid cell, whereas under the 500 m setting it may be divided into multiple adjacent grid cells. In this case, additional ambiguity may arise when determining the next traversed grid during route construction, which can in turn introduce extra uncertainty into the estimation of sailing distance. Therefore, although the 500 m grid provides slightly better predictive performance, the 1 km grid offers a more balanced trade-off between prediction accuracy, computational efficiency, and implementation robustness in the current large-scale application. As an early attempt to incorporate waterway-based route distance and traffic flow information into VAT prediction, the present study provides an initial empirical exploration of this trade-off. Further research is needed to more systematically evaluate the balance between computational cost and trajectory representation accuracy, and to develop more efficient route modeling strategies that can better preserve navigational realism while remaining computationally scalable.

To evaluate the influence of destination-point selection on VAT prediction, a sensitivity analysis is conducted using different percentile-based destination points. Since the estimated destination point is used to calculate the remaining sailing distance, its selection may affect both the distance-based benchmark and the input features used by the predictive models. Table 7 reports the prediction performance under four percentile settings. The Vessel ETA benchmark remains unchanged

Table 6
Prediction performance under different waterway network representations on the time-order test dataset.

Model	2 km grid cells				1 km grid cells				500 m grid cells				Centerline-based route			
	MAE	RMSE	R^2	MAD	MAE	RMSE	R^2	MAD	MAE	RMSE	R^2	MAD	MAE	RMSE	R^2	MAD
Vessel ETA	17.06	29.99	−0.73	5.20	17.06	29.99	−0.73	5.20	17.06	29.99	−0.73	5.20	17.06	29.99	−0.73	5.20
Estimated time	4.98	14.03	−0.02	2.26	4.98	14.03	−0.02	2.26	4.98	14.03	−0.02	2.26	4.98	14.03	−0.02	2.26
RF	5.46	14.68	0.18	2.61	5.20	13.99	0.21	2.33	5.08	13.72	0.23	2.26	5.51	15.21	0.21	2.91
LightGBM	3.72	11.41	0.57	1.56	3.53	11.03	0.61	1.41	3.45	10.95	0.63	1.37	3.56	11.01	0.61	1.51
XGBoost	3.67	11.38	0.58	1.55	**3.49**	11.04	0.69	1.40	**3.41**	**10.89**	**0.70**	**1.36**	3.55	10.80	0.62	1.41
LSTM	5.62	15.56	0.06	3.18	5.33	15.04	0.09	3.00	5.25	14.81	0.11	2.92	5.48	15.81	0.05	3.21
ANN	7.58	18.96	−0.04	3.76	7.21	18.19	−0.01	3.33	7.09	17.95	0.01	3.21	7.51	16.92	−0.05	4.01

Table 7
Prediction performance under different destination-point percentile selections on the time-order test dataset.

Model	90th percentile				80th percentile				70th percentile				60th percentile			
	MAE	RMSE	R^2	MAD	MAE	RMSE	R^2	MAD	MAE	RMSE	R^2	MAD	MAE	RMSE	R^2	MAD
Vessel ETA	17.06	29.99	−0.73	5.20	17.06	29.99	−0.73	5.20	17.06	29.99	−0.73	5.20	17.06	29.99	−0.73	5.20
Estimated time	**4.98**	14.03	−0.02	**2.26**	5.01	**13.96**	−0.01	2.31	5.19	14.38	−0.04	2.42	5.43	14.86	−0.07	2.58
RF	5.20	13.99	0.21	2.33	**5.14**	**13.92**	**0.22**	**2.30**	5.31	14.27	0.19	2.45	5.58	14.81	0.16	2.68
LightGBM	3.53	**11.03**	**0.61**	1.41	**3.50**	11.07	0.60	**1.39**	3.64	11.26	0.58	1.49	3.86	11.68	0.54	1.66
XGBoost	**3.49**	**11.04**	**0.69**	**1.40**	3.55	11.12	0.67	1.43	3.69	11.39	0.64	1.54	3.92	11.87	0.59	1.73
LSTM	**5.33**	**15.04**	**0.09**	**3.00**	5.39	15.18	0.08	3.08	5.62	15.57	0.05	3.27	5.94	16.12	0.02	3.55
ANN	**7.21**	18.19	−0.01	**3.33**	7.25	**18.06**	**0.00**	3.39	7.48	18.61	−0.03	3.58	7.86	19.27	−0.07	3.91

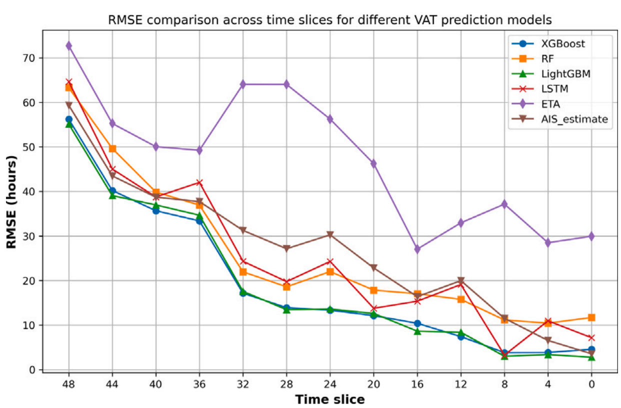

Fig. 12. RMSE error trends for different time slices.

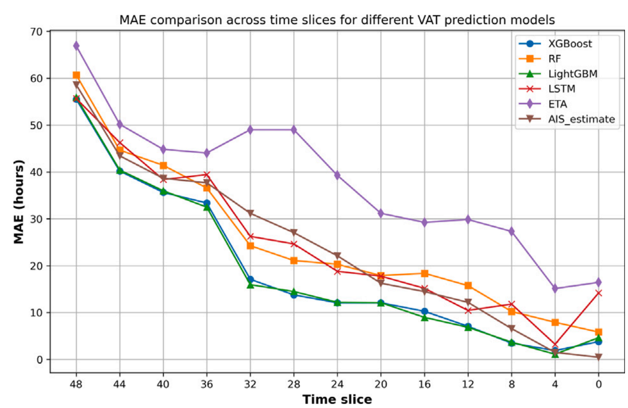

Fig. 13. MAE error trends for different time slices.

across different settings because it directly uses the ETA reported by vessels and does not depend on the estimated destination point. In contrast, the Estimated time benchmark varies across percentile settings, because changing the estimated destination point changes the calculated remaining sailing distance, and thus changes the distance-based estimated arrival time.

The results show that the prediction performance is generally stable across different percentile settings, indicating that the proposed framework is not overly sensitive to the exact destination-point selection. The 80th-percentile setting achieves the best performance for some models and metrics, such as RF and several benchmark indicators. However, the 90th-percentile setting achieves the best or comparable performance in more cases, especially for stronger prediction models such as XGBoost and LSTM. In particular, XGBoost obtains its best performance under the 90th-percentile setting, with an MAE of 3.49 h, RMSE of 11.04 h, R^2 of 0.69, and MAD of 1.40. Therefore, the 90th-percentile-based destination point is adopted in this study as a robust and effective reference for remaining-distance estimation.

To evaluate the performance of VAT prediction models at different stages of a vessel's approach to the port, the time-based test set is further divided into 49 time slices at 1-hour intervals, covering a range from 0 to 48 h before arrival. The "0-th" slice includes instances with an actual remaining time of 0 to 1 h, while the "48-th" slice contains samples with 48 h or more remaining. VAT prediction is conducted separately within each slice, allowing for a detailed assessment of model accuracy under varying temporal proximities to port arrival. The RMSE and MAE of the VAT prediction results in different time slices are visualized in Figs. 12 and 13, respectively. Figs. 12 and 13 visualize the RMSE and MAE error trends across different time slices for both VAT prediction models and benchmark methods, including vessel-reported ETA and AIS-based geometric estimates. Among the machine learning models, XGBoost, and LightGBM demonstrate superior predictive performance, with consistently lower errors across all time slices, particularly for shorter horizons. LSTM and RF exhibit greater fluctuations, indicating potential instability in certain time intervals, which may stem from its sensitivity to sequence dependencies and variations in training data. In contrast, traditional estimation methods, including ETA (vessel-reported ETA records) and AIS_estimate (derived by dividing AIS-reported distance by vessel speed), perform notably worse in long-term predictions, with significantly higher MAE and RMSE values. The high error rates associated with ETA suggest that self-reported arrival estimates may be subject to operational uncertainties, human biases, or unaccounted delays.

However, an interesting trend emerges as vessels get closer to the port: AIS_estimate, despite its overall underperformance in long-term predictions, demonstrates increasing accuracy in short-term VAT assessments, sometimes outperforming machine learning models and vessel-reported ETA. This phenomenon can be attributed to the nature of AIS-based distance evaluation, which provides a more direct measurement of a vessel's position relative to the destination. As the vessel nears the port, factors such as real-time navigation adjustments, external influences (e.g., port congestion, weather conditions), and vessel speed fluctuations have a diminished effect on distance-based estimations, making AIS-based calculations more precise. In contrast, machine learning models, while trained on historical data, may be influenced by overall trends in the dataset, leading to suboptimal performance in specific short-distance cases where real-time dynamic factors play a crucial role. The vessel-reported ETA also tends to improve as arrival nears, but its accuracy remains dependent on external factors, operational schedules, and reporting delays. The analysis underscores the effectiveness of machine learning models, particularly XGBoost and RF, in providing reliable VAT predictions across most time slices, while also highlighting the short-term reliability of AIS-based estimations as vessels approach the port. The observed error trends suggest that a hybrid approach, integrating machine learning models for long-term VAT forecasting and AIS-based estimations for short-term corrections, could further enhance practical VAT prediction accuracy in real-world maritime operations.

Overall, the analysis highlights the critical role of AIS data and the effectiveness of geometric estimations in predicting VAT. LightGBM and XGBoost stand out as the most reliable models, delivering high accuracy and robustness across various feature conditions. When using traditional random data partitioning, these models significantly reduce VAT prediction errors. However, in scenarios that simulate real port operations with data separated by time or distance, their performance declines compared to random partitioning. Nevertheless, the predictions remain substantially more accurate than vessel-reported ETAs or VAT estimates based on latitude and longitude. The findings indicate that integrating advanced machine learning models with precise geometric calculations and additional features can greatly improve the reliability of VAT predictions, especially in cases where self-reported ETAs are unreliable.

4.3. Feature importance analysis

In this subsection, the importance of different features in VAT prediction is analyzed using two complementary methods. The first is the feature importance score provided by LightGBM, which reflects the relative contribution of each feature based on its usage in decision tree splits. The second method is SHAP values, which quantify the marginal impact of each feature on the model's output, offering both global and instance-level interpretability (Lundberg and Lee, 2017). Combined, these analyses provide a comprehensive view of the role each feature plays in VAT prediction, supported by visualizations such as bar charts and force plots.

As defined in the LightGBM framework, a feature's importance is measured by the number of times it is used to split data across all trees during inference (Ke et al., 2017). A higher importance score suggests a greater influence on the model's final predictions. The top 10 features with the highest importance scores are presented in Fig. 14. The feature importance analysis in Fig. 14 reveals that "Exp_aistime" and "Exp_etatime" are the most influential features. Notably, "Exp_aistime" represents the estimated voyage remaining time calculated from the vessel's latitude and longitude, while "Exp_etatime" is derived from the vessel-reported ETA. These features highlight the critical role of temporal and spatial factors in VAT prediction. "Exp_astardistance" and "Exp_atartime also rank highly, further emphasizing the significance of spatial metrics such as remaining voyage distance and time from the A* algorithm. Traffic flow-related features (traffic_30_min, traffic_20_min, and traffic_10_min) contribute meaningfully, reflecting the impact of traffic flow and the port congestion within different time windows. Additionally, "Exp_directdistance", which represents the estimated voyage distance calculated from AIS coordinate, shows moderate importance. Environmental and vessel-specific characteristics, such as temperature, river speed, wind speed, vessel width, and length, also exhibit importance, indicating their influence on VAT prediction.

Besides, SHAP values are used to interpret the VAT prediction results from the LightGBM model, offering a clear analysis of how each feature contributes to the model's output. The SHAP summary plot visualizes the importance and impact direction of each feature, where red points indicate high feature values (larger values of the feature) and blue points represent low feature values (smaller values). This visualization highlights the most influential predictors and demonstrates how varying feature values, whether high or low, impact the VAT prediction.

The results in Fig. 15 reveal that key features such as "Exp_aistime", "Exp_astardistance", and "Exp_aistime" have the most significant influence, with higher values for these features, such as longer expected travel times or distances, being strongly associated with increased predicted VAT. Distance-related features, such as "distance_a_star" and "Node_number", also play a crucial role, indicating the importance of route length in determining arrival times. Physical attributes of the vessel, such as "Width" and "Length", contribute modestly, likely due to their indirect effects on navigational constraints or port operations. Environmental factors like "Temperature", "Wind speed", and "River speed" have a smaller but discernible impact, potentially linked to seasonal or weather-related delays. Meanwhile, traffic flow-related features, demonstrate a noticeable influence, highlighting the role of port congestion and operational delays.

Beyond the statistical interpretation of feature contributions, the SHAP analysis can also be explained in the context of physical and operational constraints in inland waterway navigation. In particular, waterway-related and environmental features influence vessels differently depending on their physical characteristics and navigational conditions. For example, water level variations can affect vessels with different drafts. Vessels with larger drafts are more sensitive to low water levels, as reduced under-keel clearance may require speed reductions, partial loading, or waiting times at critical sections, thereby increasing VAT. In contrast, smaller vessels with shallower drafts are less constrained and can maintain more stable sailing speeds under the same conditions. Similarly, traffic flow features reflect capacity constraints in narrow waterways, locks, and intersections, where high vessel density leads to queue formation and interaction delays. These effects are particularly pronounced in inland waterways due to their limited flexibility compared to open-sea navigation. The importance of distance- and time-related features, such as `Exp_aistime` and `Exp_astardistance`, is also consistent with the physical reality that travel time is fundamentally governed by remaining distance and feasible sailing speed under prevailing environmental and traffic conditions.

Overall, the analysis for feature importance and SHAP value underscores the dominant role of time and distance features in VAT prediction, with traffic conditions playing a supportive but notable role, providing a solid foundation for refining the model by prioritizing these key features. These findings not only demonstrate the effectiveness of the proposed prediction framework but also provide a foundation for deriving practical and policy-oriented recommendations, which are discussed in the following section.

5. Implications for practice and policy

The policy and managerial implications presented in this section are grounded in the empirical findings of this study. In particular, the predictive performance of the proposed models, the identified importance of AIS-based features, and the demonstrated limitations of vessel-reported ETAs provide the basis for actionable recommendations. The results show that accurate, data-driven VAT predictions can reduce uncertainty in inland waterway operations, which in turn enables more

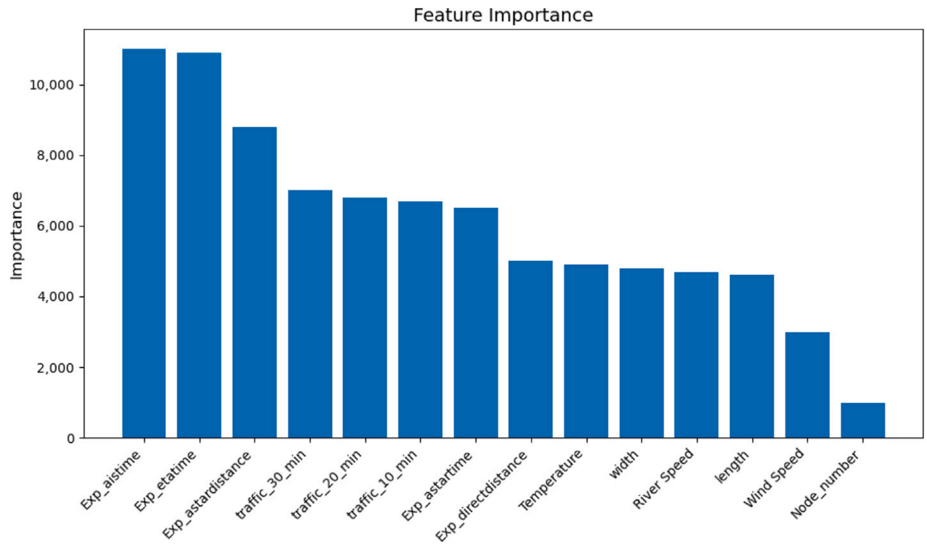

Fig. 14. Feature importance score analysis for VAT prediction.

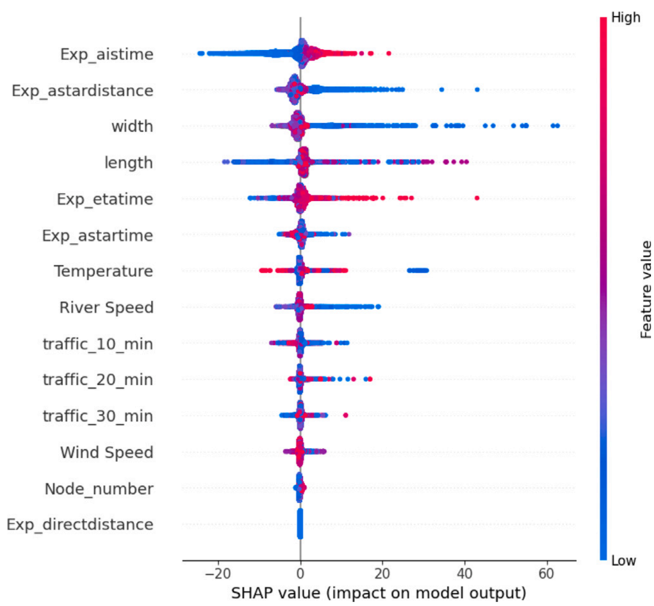

Fig. 15. Analysis of feature SHAP value.

effective planning, coordination, and policy design. Building on these findings, the following implications translate the technical contributions of this study into practical and regulatory insights for inland waterway stakeholders. By integrating AIS trajectories, vessel-reported ETAs, navigable-route distances derived from the A* algorithm, traffic flow information, and environmental variables, the model consistently outperforms both traditional geometric estimation methods and vessel-reported ETAs. These findings indicate that inland ports and waterway authorities can obtain reliable long-horizon forecasts that meaningfully support operational planning and strategic decision-making. Based on these results, several important managerial and policy implications emerge.

5.1. Managerial implications

Given the demonstrated accuracy and stability of VAT predictions, the IWT sector can operationalize these insights to enhance planning, resource allocation, and coordination across ports and waterway nodes. The following managerial implications outline how operators and logistics stakeholders can integrate predictive information into daily operations and long-term workflow redesign:

- Proactive scheduling of berths, locks, and terminal resources supported by reliable long-horizon VAT forecasts:
  Accurate VAT predictions, as demonstrated by the substantial reduction in MAE and RMSE achieved by the proposed models, create the conditions necessary for anticipatory planning. Port operators can assign berths in advance, optimize crane and labor deployment, and coordinate towage and mooring services with less uncertainty. Lock authorities can prepare operational cycles based on forecasted arrival intervals, reducing queue lengths and improving throughput. Terminal planners gain stable arrival visibility, enabling them to align yard preparation and equipment allocation with the expected workload rather than reacting to late or inaccurate information. These improvements collectively enhance operational stability and reduce inefficiencies arising from timetable uncertainty.
- Traffic-aware vessel coordination that mitigates congestion in narrow and capacity-constrained waterways:
  The integration of traffic flow features, which were shown to contribute to prediction performance, allows managers to detect congestion patterns before they manifest at critical waterway segments. With visibility on vessel density along fixed river routes, operators can stagger upstream vessel movements, manage overtaking restrictions, and adjust sequencing rules for high-density stretches. Such traffic-aware coordination reduces delay propagation, improves navigational safety, and stabilizes transit times in waterways where natural dispersion is not possible due to geometric constraints.
- Improved decision quality through automated correction of unreliable vessel-reported ETAs:
  The prediction framework significantly corrects the large inconsistencies observed in self-reported ETAs, providing a more credible reference for operational decision-making. This reduces the burden of manual verification, limits the operational risk caused by inaccurate submissions, and enables consistent planning across terminals and traffic-management centers. Over time, ports can develop performance benchmarks based on reporting accuracy, promoting more reliable ETA communication among vessel operators.
- Support for Just-in-Time (JIT) vessel arrivals that reduce waiting, fuel consumption, and emissions:

Accurate VAT forecasts provide the essential foundation for JiT arrival strategies. Vessels can adapt their speed profiles to match berth availability or lock opening times, avoiding excessive waiting at port entrances. This reduces fuel burn, lowers emission levels, and minimizes congestion near the final approach area. By harmonizing speed and arrival timing, JiT practices improve both operational efficiency and environmental performance, strengthening the sustainability of inland waterway transport.

- Enhanced coordination across ports, lock authorities, terminals, and hinterland transport partners:
  VAT predictions serve as a common informational backbone for collaborative planning. Terminals can align their operations with expected arrival windows, lock operators can synchronize opening cycles with predicted traffic surges, and hinterland transport providers can plan truck and rail transfers with greater reliability. This integrated coordination reduces mismatches between supply and handling capacities, improves the punctuality of scheduled shuttle services, and supports seamless multimodal logistics operations along key inland corridors.

5.2. Policy implications

Beyond operational improvements at the firm or terminal level, the predictive capabilities uncovered in this study offer broader opportunities for policy development. Inland waterway systems rely heavily on coordinated governance, data standards, and infrastructure support. Therefore, enhanced VAT prediction accuracy provides a foundation for policy interventions that strengthen digitalization, sustainability, and long-term competitiveness of the inland waterway sector.

- Development of standardized data-sharing frameworks for AIS, ETA, and hydrological information:
  Effective VAT prediction relies on accessible, consistent, and interoperable data. Policymakers can introduce standardized reporting formats and mandatory data-sharing requirements across vessel operators, ports, and waterway authorities. This harmonization enhances data quality, facilitates real-time model updates, and ensures equitable access to digital decision-support tools across the network.
- Introduction of incentive mechanisms to promote JIT arrival practices:
  Policy instruments can accelerate the adoption of JIT navigation. Incentives may include reduced port dues for vessels adhering to coordinated arrival windows, preferential lock access, or emission-related credits for optimized speed profiles. These measures align operator behavior with system-wide objectives related to congestion reduction and environmental sustainability.
- Support for interoperable decision-support platforms across IWT governance levels:
  Policymakers can foster the development of integrated digital platforms linking ports, lock authorities, terminal operators, and national navigation administrations. Interoperable systems ensure that predictive outputs are consistently used across the entire decision chain, reducing fragmented operations and enabling coordinated traffic and capacity management.
- Integration of predictive technologies into national modal-shift and decarbonization strategies:
  Given their demonstrated ability to reduce fuel consumption, emissions, and bottlenecks, VAT prediction systems should be embedded in long-term transport strategies aimed at shifting cargo from road to waterways. By making inland shipping more reliable and efficient, predictive analytics can enhance its competitiveness and contribute to national sustainability and climate objectives.

6. Conclusion

This study addresses a critical gap in the prediction of VAT for IWT, which is increasingly important due to the growing reliance on inland waterways as a sustainable mode of cargo transport. Previous research primarily focused on VAT prediction for ocean-going vessels, often using simplified distance-based estimations and data from a single source, such as AIS or other static information. Additionally, studies specifically addressing VAT prediction for IWT rarely account for the unique characteristics of IWT, such as varying traffic conditions, waterway infrastructure, and regional factors.

To fulfill such a research gap, we propose a VAT data processing and prediction framework using a combination of AIS data, as well as additional contextual features, such as ETA records, vessel physical dimensions, weather conditions, and traffic flow patterns.

The results demonstrate a substantial improvement in VAT prediction accuracy compared to vessel-reported ETAs. In particular, the proposed approach reduces the mean absolute error from 17.06 h to 3.49 h, corresponding to an improvement of approximately 80%, while maintaining strong predictive robustness across different experimental settings. Tree-based models, particularly LightGBM and XGBoost, consistently achieve the best performance. Feature importance analysis further highlights that temporal and spatial features derived from AIS data are the most influential predictors, while traffic flow and waterway characteristics provide additional explanatory power.

Our findings contribute to the existing research by shifting the focus from ocean-going VAT prediction to IWT, which consider the unique characteristics of IWT, and by innovatively incorporating multiple data sources. Thus, this work highlights the value of incorporating multisource data, including waterway characteristics, traffic flow, vessel-reported ETA records, and weather information, into VAT prediction models for IWT. Furthermore, it provides a further innovation in applying the A* algorithm to segment inland waterways and estimate the remaining route distance, which improves the accuracy of VAT predictions. Building on these predictive advances, this study not only demonstrates the operational benefits of multisource data integration but also provides actionable insights for practice and governance. The improved VAT predictions form the analytical basis for the managerial implications and policy recommendations proposed in this work, which guide ports, waterway authorities, and regulators in leveraging predictive analytics for more efficient resource planning, congestion mitigation, and sustainable inland waterway management.

This work lays the foundation for optimizing port operations, improving berth Throughput, and contributing to more efficient port management systems. By enabling real-time Just-in-Time vessel arrival predictions, it helps reduce unnecessary waiting times and idle periods for vessels, thereby minimizing fuel consumption and emissions. This, in turn, supports more sustainable and environmentally-friendly port operations, contributing to reduced carbon footprints and more efficient use of resources. Additionally, the ability to predict VAT more accurately facilitates better planning for berth allocation, further enhancing operational efficiency and reducing congestion at port terminals.

While this study provides valuable insights and lays the groundwork for VAT prediction in IWT, several limitations should be acknowledged. First, the dataset used in this study primarily focuses on the Port of Rotterdam, which may limit the direct applicability of the findings to other ports with different operational characteristics, such as tidal constraints or traffic control rules. Second, the predictive model developed in this study is designed as an effective and operationally applicable VAT prediction framework rather than a purely new machine-learning architecture. Its main innovation lies in integrating reported ETA, AIS-derived movement information, traffic-flow characteristics, and network-based remaining-distance features to improve VAT prediction in inland waterway transportation. This design enables the model to capture vessel movement dynamics and waterway traffic conditions more effectively than traditional ETA-based or purely AIS-based methods. Third, the A* algorithm adopted in this study to estimate the remaining sailing distance is based on a simplified and discretized representation of the waterway network using 1 km grid cells. While this approach provides a computationally efficient approximation for large-scale feature construction, it does not fully capture detailed navigable centerlines, channel bends, or bank-related navigation constraints in real inland waterway systems. In addition, it does not explicitly account for route choice heterogeneity across vessels, operators, or dynamic traffic management conditions. As a result, some discrepancy may exist between the approximated remaining sailing distance and the actual navigational path followed by vessels in practice.

Future research should seek to expand this work by applying the models to multiple ports or interconnected waterway networks, which would improve the generalizability of the findings. Incorporating additional operational constraints, such as lock times, traffic signals, tidal restrictions, and other traffic control rules, could further enhance the accuracy and practical relevance of the prediction models. In addition, more realistic and adaptive route modeling strategies should be investigated to better capture actual vessel movement and route choice heterogeneity in inland waterway transport. Future studies could also explore higher-resolution network representations or centerline-based navigable routes to achieve a better balance between trajectory representation accuracy and computational efficiency. Finally, real-time models with adaptive retraining capabilities should be explored to improve the robustness of VAT predictions under changing environmental and traffic conditions, thereby further advancing the practical applicability of VAT prediction systems and contributing to smarter and more resilient port management solutions.

CRediT authorship contribution statement

Peter Wenzel: Writing – review & editing, Writing – original draft, Software, Resources, Methodology, Data curation. **Zhong Chu:** Writing – review & editing, Writing – original draft, Visualization, Software, Methodology, Data curation, Conceptualization. **Frederik Schulte:** Writing – review & editing, Supervision, Resources, Project administration, Investigation, Funding acquisition.

Declaration of competing interest

The authors declare that they have no known competing financial interests or personal relationships that could have appeared to influence the work reported in this paper.

Acknowledgements

The authors gratefully acknowledge the support from the Graduate School of The Hong Kong Polytechnic University through the Research Student Attachment Programme. This research was supported by the Research Grants Council (RGC) of Hong Kong under the Junior Research Fellow Scheme (JRFS) (Grant No. JRFS2627-5H02).

Appendix. Hyperparameter tuning details

To ensure a fair and reproducible comparison, the hyperparameters of all compared machine learning models are tuned using grid search combined with cross-validation. Grid search is a systematic strategy that evaluates all candidate combinations from a predefined hyperparameter set and selects the one that yields the best validation performance. Compared with manual trial-and-error, this approach provides a more objective and transparent tuning procedure. In this study, 5-fold cross-validation is adopted on the training set during the hyperparameter tuning process. Specifically, the training data is partitioned into five subsets of approximately equal size. In each round, four subsets are used for model training and the remaining one is used for validation, until every subset serves once as the validation set. The average validation performance across the five folds is then used as the criterion for model selection. This procedure reduces the risk of overfitting to a single validation split and improves the robustness of the selected hyperparameter configuration.

The compared models in this study include RF, LightGBM, XGBoost, LSTM, and ANN. Since two different data partition strategies are considered in the main experiments, namely the time-based split and the voyage-based split, the hyperparameter tuning procedure is conducted separately for each setting. In other words, for each model, hyperparameter optimization is performed twice based on the corresponding training set under the two split strategies, so that the selected configurations are better matched to the characteristics of each prediction scenario.

For tree-based models, the main hyperparameters to be tuned include the number of estimators, the maximum tree depth, the minimum number of samples required for node splitting, and the learning rate when applicable. Specifically, for RF, the tuning mainly focuses on the number of trees, maximum depth, minimum samples split, and minimum samples leaf. For LightGBM, the key hyperparameters include the number of estimators, learning rate, maximum depth, number of leaves,

Table A.8
Hyperparameter search ranges and final selected settings for RF.

Hyperparameter	Search range	Time-based split	Voyage-based split
n_estimators	{100, 200, 300, 400, 500}	400	400
max_depth	{5, 10, 15, 20, None}	15	20
min_samples_split	{2, 5, 10}	5	5
min_samples_leaf	{1, 2, 3, 4}	2	3
max_features	{sqrt, log2, None}	None	None

Table A.9
Hyperparameter search ranges and final selected settings for LightGBM.

Hyperparameter	Search range	Time-based split	Voyage-based split
n_estimators	{100, 200, 300, 400, 500}	400	500
learning_rate	{0.01, 0.05, 0.1}	0.1	0.1
max_depth	{5, 10, 15, −1}	15	−1
num_leaves	{15, 31, 63, 127}	63	127
min_child_samples	{10, 20, 30, 50}	20	20
subsample	{0.6, 0.8, 1.0}	1.0	1.0
colsample_bytree	{0.6, 0.8, 1.0}	0.8	0.8

Table A.10
Hyperparameter search ranges and final selected settings for XGBoost.

Hyperparameter	Search range	Time-based split	Voyage-based split
n_estimators	{100, 200, 300, 400, 500}	400	500
learning_rate	{0.01, 0.05, 0.1}	0.1	0.1
max_depth	{3, 5, 7, 9}	5	7
subsample	{0.6, 0.8, 1.0}	1.0	1.0
colsample_bytree	{0.6, 0.8, 1.0}	1.0	1.0
gamma	{0, 0.1, 0.3}	0.3	0.1
reg_lambda	{1, 5, 10}	5	10

Table A.11
Hyperparameter search ranges and final selected settings for ANN.

Hyperparameter	Search range	Time-based split	Voyage-based split
hidden_layers	{1, 2, 3}	3	3
hidden_units	{32, 64, 128, 256}	256	256
dropout	{0.0, 0.2, 0.5}	0.5	0.5
batch_size	{16, 32, 64}	32	64
learning_rate	{0.001, 0.0005, 0.0001}	0.001	0.001
epochs	{50, 100, 150}	100	100
activation	{ReLU, Tanh}	ReLU	ReLU

and minimum child samples. For XGBoost, the main tuned hyperparameters include the number of estimators, learning rate, maximum depth, subsample ratio, and column sampling ratio.

For deep learning models, the main hyperparameters are related to network architecture and optimization settings. For LSTM, the tuned hyperparameters mainly include the number of hidden units, number of LSTM layers, dropout rate, batch size, learning rate, and number of training epochs. For ANN, the main tuned hyperparameters include the number of hidden layers, number of neurons in each layer, dropout rate, batch size, learning rate, and number of training epochs.

The detailed search ranges and the final selected hyperparameter settings for all models under the two data split strategies are summarized in the following tables (see Tables A.8–A.11).

Data availability

Data will be made available on request.

References

Chen, T., Guestrin, C., 2016. Xgboost: A scalable tree boosting system. In: Proceedings of the 22nd Acm Sigkdd International Conference on Knowledge Discovery and Data Mining. pp. 785–794.

Chu, Z., Yan, R., Wang, S., 2024. Evaluation and prediction of punctuality of vessel arrival at port: a case study of Hong Kong. Marit. Policy & Manag. 51 (6), 1096–1124.

Chu, Z., Yan, R., Wang, S., 2025. Vessel arrival time to port prediction via a stacked ensemble approach: Fusing port call records and AIS data. Transp. Res. Part C: Emerg. Technol. 176, 105128.

Chu, Z., Yan, R., Yang, X., Pang, K.-W., Wang, S., 2026. Integrating vessel arrival time forecasting into berth allocation decisions: A predictive-operational framework. Adv. Eng. Informatics 69, 104010.

Dobrkovic, A., Iacob, M.-E., Van Hillegersberg, J., 2016. Maritime pattern extraction from AIS data using a genetic algorithm. In: 2016 IEEE International Conference on Data Science and Advanced Analytics. DSAA, IEEE, pp. 642–651.

El Mekkaoui, S., Benabbou, L., Berrado, A., 2023. Deep learning models for vessel's ETA prediction: bulk ports perspective. Flex. Serv. Manuf. J. 35 (1), 5–28.

Emmens, T., Amrit, C., Abdi, A., Ghosh, M., 2021. The promises and perils of automatic identification system data. Expert Syst. Appl. 178, 114975.

Fan, T., Chen, D., Huang, C., 2023. Contextualized spatial–temporal network for inland vessel travel time prediction based on AIS data. In: 2023 7th International Conference on Transportation Information and Safety. ICTIS, IEEE, pp. 1–7.

Filom, S., Amiri, A.M., Razavi, S., 2022. Applications of machine learning methods in port operations–a systematic literature review. Transp. Res. Part E: Logist. Transp. Rev. 161, 102722.

Grinsztajn, L., Oyallon, E., Varoquaux, G., 2022. Why do tree-based models still outperform deep learning on typical tabular data? Adv. Neural Inf. Process. Syst. 35, 507–520.

Halpe, P., Adams, M., Walker, T.R., 2025. Challenges and opportunities for ports in achieving net-zero emissions in maritime transport. Transp. Res. Interdiscip. Perspect. 30, 101379.

Hart, P.E., Nilsson, N.J., Raphael, B., 1968. A formal basis for the heuristic determination of minimum cost paths. IEEE Trans. Syst. Sci. Cybern. 4 (2), 100–107.

Havenbedrijf Rotterdam B.V., 2023. Highlights annual report 2023. (Accessed 7 January 2025) https://reporting.portofrotterdam.com/FbContent.ashx/pub_1018/downloads/v240305112534/PoR_AR_2023_Annual_Report_Highlights.pdf.

Jiang, S., Liu, L., Peng, P., Xu, M., Yan, R., 2025. Prediction of vessel arrival time to port: a review of current studies. Marit. Policy & Manag. 1–26.

Jin, C.-J., Yang, W., Jiang, R., Liao, P., Zheng, S., Wang, H., 2023. Vessel-following dynamics: Experiment and modeling. Phys. A 615, 128588.

Ke, G., Meng, Q., Finley, T., Wang, T., Chen, W., Ma, W., Ye, Q., Liu, T.-Y., 2017. Lightgbm: A highly efficient gradient boosting decision tree. Adv. Neural Inf. Process. Syst. 30.

Kim, S., Kim, H., Park, Y., 2017. Early detection of vessel delays using combined historical and real-time information. J. Oper. Res. Soc. 68 (2), 182–191.

Kim, J.S., Park, H.J., Shin, W., Park, D., Han, S.W., 2023. WAY: estimation of vessel destination in worldwide AIS trajectory. IEEE Trans. Aerosp. Electron. Syst. 59 (5), 5961–5977.

Last, P., Hering-Bertram, M., Linsen, L., 2019. Interactive history-based vessel movement prediction. IEEE Intell. Syst. 34 (6), 3–13.

Lei, J., Chu, Z., Wu, Y., Liu, X., Luo, M., He, W., Liu, C., 2024. Predicting vessel arrival times on inland waterways: A tree-based stacking approach. Ocean Eng. 294, 116838.

Li, H., Jiao, H., Yang, Z., 2023a. AIS data-driven ship trajectory prediction modelling and analysis based on machine learning and deep learning methods. Transp. Res. Part E: Logist. Transp. Rev. 175, 103152.

Li, H., Jiao, H., Yang, Z., 2023b. Ship trajectory prediction based on machine learning and deep learning: A systematic review and methods analysis. Eng. Appl. Artif. Intell. 126, 107062.

Lundberg, S.M., Lee, S.-I., 2017. A unified approach to interpreting model predictions. Adv. Neural Inf. Process. Syst. 30.

Noman, A.A., Heuermann, A., Wiesner, S.A., Thoben, K.-D., 2021. Towards data-driven gru based eta prediction approach for vessels on both inland natural and artificial waterways. In: 2021 IEEE International Intelligent Transportation Systems Conference. ITSC, IEEE, pp. 2286–2291.

Nosar, N.S., 2025. Unraveling interactions: Mechanisms shaping the transition of small and medium-sized ports to energy hubs. Transp. Res. Interdiscip. Perspect. 31, 101417.

Ogura, T., Inoue, T., Uchihira, N., 2021. Prediction of arrival time of vessels considering future weather conditions. Appl. Sci. 11 (10), 4410.

Park, K., Sim, S., Bae, H., 2021. Vessel estimated time of arrival prediction system based on a path-finding algorithm. Marit. Transp. Res. 2, 100012.

Perra, V.-M., Boile, M., 2026. Envisioning AI for international cooperation in maritime transport: conceptual insights from short sea shipping and maritime spatial planning. Transp. Res. Interdiscip. Perspect. 36, 101819.

Qiang, H., Xie, S., Guo, Z., Peng, X., 2023. SocialVessel: VAE-inspired multi-vessel gated recurrent units for vessel trajectory prediction in port areas. In: 2023 IEEE 26th International Conference on Intelligent Transportation Systems. ITSC, IEEE, pp. 4504–4509.

Saafi, M.A., Traver, M., Hamad, E., 2025. Towards maritime transport decarbonization: Comparison of onboard carbon capture and storage to low carbon alternative fuels. Transp. Res. Interdiscip. Perspect. 32, 101494.

Štepec, D., Martinčič, T., Klein, F., Vladušič, D., Costa, J.P., 2020. Machine learning based system for vessel turnaround time prediction. In: 2020 21st IEEE International Conference on Mobile Data Management. MDM, IEEE, pp. 258–263.

Ta, A.S., Le, L.T., Bui-Duy, L., 2025. Toward decarbonization in the sea transport of biomass pellet supply chain: An application of artificial neural network embedded routing optimization. Transp. Res. Interdiscip. Perspect. 34, 101759.

Viellechner, A., Spinler, S., 2020. Novel data analytics meets conventional container shipping: predicting delays by comparing various machine learning algorithms.

Wenzel, P., Jovanovic, R., Schulte, F., 2023. A neural network approach for ETA prediction in inland waterway transport. In: International Conference on Computational Logistics. Springer, pp. 219–232.

Wu, X., Roy, U., Hamidi, M., Craig, B.N., 2020. Estimate travel time of ships in narrow channel based on AIS data. Ocean Eng. 202, 106790.

Xiong, S., Tang, C., Zhang, Y., Xiong, H., Xu, Y., Shimada, A., 2025. Enhancing nonlinear dependencies of mamba via negative feedback for time series forecasting. Appl. Soft Comput. 113758.

Xu, X., Liu, C., Li, J., Miao, Y., 2022. Trajectory clustering for SVR-based time of arrival estimation. Ocean Eng. 259, 111930.

Yang, W., Jiang, S., Liao, P., Wang, H., 2023. Evaluation of car-following model for inland vessel-following behavior. Ocean Eng. 284, 115196.

Yang, W., Liao, P., Jiang, S., Wang, H., 2025. Analysis of vessel traffic flow characteristics in inland restricted waterways using multi-source data. Ocean Eng. 317, 120065.

Yang, T.-Y., Zou, L., Wu, Z.-X., Chen, W.-M., 2025. An improved A-star algorithm coupled with graph division and AIS data for ship path planning. Ocean Eng. 330, 121234.

Zhang, X., Fu, X., Xiao, Z., Xu, H., Wei, X., Koh, J., Ogawa, D., Qin, Z., 2023. Prediction of vessel arrival time to pilotage area using multi-data fusion and deep learning. In: 2023 IEEE 26th International Conference on Intelligent Transportation Systems. ITSC, IEEE, 2268–2268.

Zhang, Y., Guan, R., Li, L., Yang, R., Yue, Y., Lim, E.G., 2025a. Radarode: An ODE-embedded deep learning model for contactless ecg reconstruction from millimeter-wave radar. IEEE Trans. Mob. Comput..

Zhang, T., Yin, J., Wang, X., Min, J., 2024. Prediction of container port congestion status and its impact on ship's time in port based on AIS data. Marit. Policy & Manag. 51 (5), 669–697.

Zhang, Y., Zhao, H., Xiong, S., Yang, R., Lim, E.G., Yue, Y., 2025b. From high-SNR radar signal to ECG: A transfer learning model with cardio-focusing algorithm for scenarios with limited data. IEEE Trans. Mob. Comput..

Zhou, Z.-H., 2021. Machine Learning. Springer nature.